Contribution from the Department of Chemistry,
The University of Michigan, Ann Arbor, Michigan 48109-1055

Reactivity of the Mo(S_x) Functional Groups in Thio- and Oxothiomolybdate Complexes toward Carbon Disulfide. Synthesis and Reactivity of Trithio- and Perthiocarbonate Complexes of Mo(IV) and Mo(V) and Structural Characterization of *trans*-$[Ph_4P]_2[Mo(S)(CS_4)_2]\cdot DMF$ (I), *cis*-$[Ph_4P][Et_4N][Mo(S)(CS_4)_2]$ (II), *cis-syn*-$[Ph_4P]_2[Mo_2(S)_2(\mu\text{-}S)_2(CS_4)_2]\cdot{}^1/_2DMF$ (III), *syn*-$[Ph_4P]_2[Mo_2(S)_2(\mu\text{-}S)_2(CS_3)_2]$ (IV), and *syn*-$[Et_4N]_2[Mo_2(O)_2(\mu\text{-}S)_2(CS_4)(CS_3)]$ (V)

D. Coucouvanis,* M. E. Draganjac, S. M. Koo, A. Toupadakis, and A. I. Hadjikyriacou

Received July 26, 1991

The syntheses and structures of the diamagnetic complexes *trans*-$[Ph_4P]_2[Mo(S)(CS_4)_2]\cdot DMF$ (I), *cis*-$[Ph_4P][Et_4N][Mo(S)(CS_4)_2]$ (II), *cis-syn*-$[Ph_4P]_2[Mo_2(S)_2(\mu\text{-}S)_2(CS_4)_2]\cdot{}^1/_2DMF$ (III), *syn*-$[Ph_4P]_2[Mo_2(S)_2(\mu\text{-}S)_2(CS_3)_2]$ (IV), and *syn*-$[Et_4N]_2[Mo_2(O)_2(\mu\text{-}S)_2(CS_4)(CS_3)]$ (V) and the syntheses of *syn*-$[Et_4N]_2[Mo_2(O)_2(\mu\text{-}S)_2(\eta^2\text{-}S_4)(\eta^2\text{-}CS_3)]$ (VI), *syn*-$[Et_4N]_2[Mo_2(O)_2(\mu\text{-}S)_2(\eta^2\text{-}S_2)(\eta^2\text{-}CS_3)]$ (VII), and *syn*-$[Et_4N]_2[Mo_2(O)_2(\mu\text{-}S)_2(\eta^2\text{-}CS_3)_2]$ (VIII) are reported. Compounds I, II and V crystallize in the space groups $P2_1/a$, *Pbcm*, and *Pnca*, respectively. Compounds III and IV both crystallize in the space group $P\bar{1}$. The cell dimensions are as follows. I: a = 19.769 (7) Å, b = 13.345 (5) Å, c = 21.647 (8) Å, β = 111.21 (3)°, Z = 4. II: a = 8.024 (2) Å, b = 18.371 (5) Å, c = 27.183 (5) Å, $\alpha = \beta = \gamma$ = 90°, Z = 4. III: a = 10.748 (3) Å, b = 12.262 (4) Å, c = 22.377 (7) Å, α = 75.66 (3)°, β = 87.70 (2)°, γ = 80.49 (3)°, Z = 2. IV: a = 10.655 (3) Å, b = 13.720 (5) Å, c = 19.764 (5) Å, α = 90.90 (3)°, β = 102.43 (2)°, γ = 112.08 (2)°, Z = 2. V: a = 13.005 (4) Å, b = 31.879 (8) Å, c = 15.540 (4) Å, $\alpha = \beta = \gamma$ = 90°, Z = 8. Crystallographic data for the four structures were obtained on an automatic diffractometer employing Mo Kα radiation. The refinement of the structures by full-matrix least-squares methods was based on 2622 unique reflections ($2\theta_{max}$ = 40°, $I > 3\sigma(I)$) for I, on 1424 unique reflections ($2\theta_{max}$ = 40°, $I > 3\sigma(I)$) for II, on 2648 unique reflections ($2\theta_{max}$ = 40°, $I > 3\sigma(I)$) for III, on 3998 unique reflections ($2\theta_{max}$ = 45°, $I > 3\sigma(I)$) for IV, and on 2160 unique reflections ($2\theta_{max}$ = 45°, $I > 3\sigma(I)$) for V. Anisotropic temperature factors were used for all non-hydrogen atoms in I-V. At the current stage of refinement on 339 parameters for I, 148 parameters for II, 371 parameters for III, 578 parameters for IV, and 256 parameters for V with all atoms present in the asymmetric units, R_w = 0.055, 0.081, 0.075, 0.030, and 0.078, respectively. The structures of the isomeric complex anions in I and II show the Mo(IV) ions in square pyramidal coordination with two CS_4^{2-} ligands in the equatorial plane (trans to each other for I and cis for II) and a terminal sulfido axial ligand lying ~0.7 Å above the equatorial plane. The $[Mo_2(\mu\text{-}S)_2(S)_2(L)_2]^{2-}$ dimeric units in III and IV contain the $[Mo_2(\mu\text{-}S)_2(S)_2]^{2+}$ cores with five-coordinate Mo(V) ions, the Mo=S units in the syn configuration, and L = CS_4^{2-} terminal ligands in III and L = CS_3^{2-} terminal ligands in IV. The structure of V shows a dimeric asymmetric anion that is a "mixed-ligand" analogue of III and IV with one CS_3^{2-} and one CS_4^{2-} as terminal ligands and Mo=O units in place of the Mo=S units. Selected structural features for I and II include the following: Mo=S, 2.126 (3) and 2.127 (4) Å; Mo-S_L, 2.383 (3) and 2.376 (3) Å; Mo-S-S_L, 2.326 (3) and 2.320 (3) Å. Selected structural features for III: Mo-Mo, 2.840 (3) Å; Mo-S_b, 2.316 (5) Å; Mo=S, 2.108 (5) Å; Mo-S_b-Mo, 75.6°; S_b-Mo-S_b, 101.4°. The Mo-Mo distance in IV is found at 2.823 (1) Å and in V at 2.835 (2) Å. Other selected structural features of IV and V: Mo-S_b, 2.300 (7) and 2.305 (5) Å; Mo-S_b-Mo, 75.6 and 75.4°; S_b-Mo-S_b, 100.8 and 100.5°. The Mo=S bond length in IV is 2.100 (2) Å, and the Mo=O bond length in V is 1.68 (1) Å. A study of the ^{13}C NMR spectra of the perthio- and trithiocarbonate complexes shows that the complicated solution behavior of these complexes is dominated by sulfur addition and CS_2 elimination reactions.

Introduction

In recent reports[1,2] we have identified a number of specific "functional groups" in the various molybdothio anions that are characterized by distinct reactivity properties. It is now well established that in the thiomolybdate complexes both the Mo-η^2-S_x and Mo=S groups are sufficiently nucleophilic to attack electrophilic molecules such as dicarboalkoxyacetylenes,[1-3] CS_2,[4] or SO_2.[5] Detailed synthetic and crystallographic studies have shown that the reactions of the $[(S_4)_2Mo^{IV}{=}S]^{2-}$, $[(S_4)(S)Mo^{V}(\mu\text{-}S)_2Mo^{V}(S)(S_2)]^{2-}$, and $[(L)(O)Mo^{V}(\mu\text{-}S)_2Mo^{V}(O)(S_x)]^{2-}$ complexes with dicarbomethoxyacetylene (DMA) proceed until all S_x^{2-} sulfido ligands (with the exception of the μ-S^{2-} ligands) are converted into the dithiolene (DMAD) ligands.[1,2] The initial step in these reactions is difficult to ascertain, but it could be electrophilic attack by DMA followed by addition into the Mo=S bonds or insertion into the Mo—η^2-S_2 bonds. The later reaction has been demonstrated already in the synthesis of the first vinyl disulfide complex.[3a] The reactive vinyl sulfide or vinyl disulfide ligands eventually transform to dithiolenes. Spectroscopic (^1H NMR) evidence suggests that this transformation may occur for the Mo-coordinated vinyl sulfide by insertion of S into the Mo-C bond and for the Mo-vinyl disulfide complex by a S-catalyzed isomerization reaction.[1-2,6]

The superior reactivity of the Mo=S and Mo-η^2-S_2 groups toward electrophiles, relative to that of the Mo-η^2-S_4 group in similar reactions, is aptly demonstrated in the relative reactivities of the $[(S_4)_2Mo^{IV}{=}O]^{2-}$ and $[(S_4)_2Mo^{IV}{=}S]^{2-}$ complexes toward CS_2. The latter readily reacts with CS_2 to give both *cis*- and *trans*-$[(CS_4)_2Mo^{IV}{=}S]^{2-}$ complexes.[4,7] By comparison, the $[(S_4)_2Mo^{IV}{=}O]^{2-}$ complex is unreactive toward CS_2 unless it is activated by Ph_3P.[8] Presumably, Ph_3P promotes the generation of reactive η^2-S_2 units from the Mo-coordinated η^2-S_4 ligands.

A remarkable characteristic of the Mo-η^2-CS_4 groups is their ability to reversibly release CS_2 and revert to Mo-η^2-S_2. On the basis of this observation,[7] we have suggested previously[2] that under certain conditions the Mo-η^2-S_2 functional group may be directly involved in the activation of C-S bonds in saturated or unsaturated sulfur-containing organic molecules in the catalysis of the hydrodesulfurization (HDS) reaction.[9] Our research efforts in recent years have been directed toward an understanding of the comparative reactivities of the Mo=S and Mo-η^2-S_2 groups in soluble

(1) Coucouvanis, D.; Hadjikyriacou, A. I.; Draganjac, M. E.; Kanatzidis, M. G.; Ileperuma, O. *Polyhedron* **1986**, *5*, 349.
(2) (a) Coucouvanis, D.; Hadjikyriacou, A. I.; Toupadakis, A.; Koo, Sang-Man; Ileperuma, O.; Draganjac, M. E.; Saligoglou, A. *Inorg. Chem.* **1991**, *30*, 754. (b) Coucouvanis, D.; Toupadakis, A.; Lane, J. D.; Koo, Sang-Man; Kim, C. G.; Hadjikyriacou, A. I. *J. Am. Chem. Soc.* **1991**, *113*, 5271.
(3) (a) Halbert, T. R.; Pan, W. H.; Stiefel, E. I. *J. Am. Chem. Soc.* **1983**, *105*, 5476. (b) Bolinger, C. M.; Rauchfuss, T. B. *Inorg. Chem.* **1982**, *21*, 3947.
(4) Coucouvanis, D.; Draganjac, M. E. *J. Am. Chem. Soc.* **1982**, *104*, 6820.
(5) Kim, C. G.; Coucouvanis, D. Manuscript in preparation.
(6) Coucouvanis, D.; Toupadakis, A.; Koo, Sang-Man; Hadjikyriacou, A. I. *Polyhedron* **1989**, *8*, 1705-1716.
(7) Draganjac, M. E. Ph.D. Thesis, University of Iowa, 1983.
(8) Toupadakis, A. Ph.D. Thesis, University of Michigan, 1990.
(9) (a) Massoth, F. E. *Adv. Catal.* **1978**, *27*, 265. (b) Topsoe, J.; Clausen, B. S. *Catal. Rev.—Sci. Eng.* **1984**, *26*, 395. (c) Weisser, O.; Landa, S. *Sulfide Catalysts: Their Properties and Applications*; Pergamon Press: London, 1973.

0020-1669/92/1331-1186$03.00/0

molybdenum sulfide complexes.

In this paper, we report in detail on the reactivity of certain sulfidomolybdenum complexes toward CS_2 and on the solution behavior of the derivative CS_3^{2-} and CS_4^{2-} complexes. The crystal and molecular structures of the complexes $[Ph_4P]_2[trans\text{-}(S)Mo(\eta^2\text{-}CS_4)_2]\cdot DMF$ (I), $[Ph_4P][Et_4N][cis\text{-}(S)Mo(\eta^2\text{-}CS_4)_2]$ (II), $[Ph_4P]_2[syn\text{-}cis\text{-}Mo_2(S)_2(\mu\text{-}S)_2(\eta^2\text{-}CS_4)_2]\cdot{}^1/_2DMF$ (III), $[Ph_4P]_2[syn\text{-}Mo_2(S)_2(\mu\text{-}S)_2(\eta^2\text{-}CS_3)_2]$ (IV), and $[Et_4N]_2[Mo_2(O)_2(\mu\text{-}S)_2(\eta^2\text{-}CS_4)(\eta^2\text{-}CS_3)]$ (V) also are reported in detail. Of these, I–III have been reported briefly in a previous communication.[4]

Experimental Section

Synthesis. The chemicals in this work were used as purchased. Acetonitrile (CH_3CN), dichloromethane (CH_2Cl_2), and diethyl ether were distilled over calcium hydride. All syntheses using oxothiomolybdate complexes were carried out under air. Those with thiomolybdate complexes were carried out in an inert atmosphere using a Vacuum Atmosphere Dri-Lab glovebox filled with prepurified nitrogen, unless otherwise specified.

Bis(tetraphenylphosphonium) *trans*-Bis(η^2-perthiocarbonato)thiomolybdate(IV) Dimethylformamide Monosolvate, $[Ph_4P]_2[trans\text{-}(S)Mo(\eta^2\text{-}CS_4)_2]\cdot DMF$ (I). An amount of $[Ph_4P]_2[(S)Mo(\eta^2\text{-}S_4)_2]$[10] (0.3 g, 0.28 mmol) was dissolved in 40 mL of distilled DMF. To this solution was added 40 mL of CS_2, and the solution was stirred for 5 min. A change in color from brown to orange occurred, and at this stage, diethyl ether was added to the solution to incipient crystallization. After the mixture was allowed to stand for 12 h, the product formed as red-orange crystals and was isolated by filtration and washed with several 30-mL portions of diethyl ether. The weight of the product after drying in air was 0.21 g (75% yield). On occasion, an oil resulted after the addition of ether. In such a case the oil was allowed to stand in contact with the solution for 3–5 days. Invariably the oil crystallized to red orange crystals. Anal. Calcd for $C_{53}H_{47}P_2MoS_9NO$ (fw = 1159): C, 54.82; H, 4.06; Mo, 8.28; S, 24.35; P, 5.35. Found: C, 54.79; H, 4.26; Mo, 7.79; S, 24.48; P, 5.26. FT-IR (KBr pellet; cm^{-1}): ν(C=S) 980 (s). UV–vis (DMF solution, 10^{-3} M; nm): 334 (sh), 430 (sh).

Bis(tetraphenylphosphonium) *cis*-Bis(η^2-perthiocarbonato)thiomolybdate(IV), $[Ph_4P]_2[cis\text{-}(S)Mo(\eta^2\text{-}CS_4)_2]$. An amount of $[Ph_4P]_2[(S)Mo(\eta^2\text{-}S_4)_2]$[10] (0.3 g, 0.28 mmol) was dissolved in 40 mL of distilled DMF. To this solution was added 40 mL of CS_2 along with four to eight drops of water. The solution was stirred for 5 min, and 20 mL of absolute ethanol was added. At this stage, an excess of diethyl ether was added to force the product out of solution as a yellow-brown oil. Upon standing in contact with the mother liquor (3–5 days), the oil solidified to golden yellow flakes. These were isolated by filtration and washed with several portions of diethyl ether. The weight after air drying was 0.20 g (75% yield). Anal. Calcd for $C_{50}H_{40}P_2MoS_9$ (fw = 1086): C, 55.75; H, 3.68; Mo, 8.84; S, 26.52; P, 5.71. Found: C, 54.76; H, 4.09; Mo, 8.64; S, 25.69; P, 5.40. FT-IR (KBr pellet; cm^{-1}): ν(C=S) 977 (s). UV–vis (DMF solution, 10^{-3} M; nm): 335, 393, 430 (sh).

Tetraethylammonium Tetraphenylphosphonium *cis*-Bis(η^2-perthiocarbonato)thiomolybdate(IV), $[Ph_4P][Et_4N][cis\text{-}(S)Mo(\eta^2\text{-}CS_4)_2]$ (II). An amount of $[Et_4N]_2[(S)Mo(\eta^2\text{-}S_4)_2]$[10] (0.2 g, 0.3 mmol) was dissolved in 50 mL of distilled DMF. To this solution was added 50 mL of CS_2 with stirring. After 5 min, 0.23 g (0.6 mmol) of Ph_4PCl was added under stirring. To the solution were added 10 mL of absolute ethanol and then diethyl ether (ca. 200 mL) to incipient crystallization. The solution was allowed to stand for ca. 3 days, at which time a mixture of orange-red crystalline clusters and long black needles formed; these were isolated by filtration. The orange-red crystals were characterized by electronic spectroscopy as containing the *trans*-$[(S)Mo(\eta^2\text{-}CS_4)_2]$ isomer. The dark needles were found to contain the anion as the cis isomer, as verified by a single-crystal X-ray structure determination. The relative yields were 40% for the trans and 60% for the cis isomers. Anal. Calcd for $C_{34}H_{40}PNMoS_9$ (fw = 877): C, 46.47; H, 4.56; Mo, 10.93; S, 32.80; P, 3.53; N, 1.59. Found (for the black needles): C, 46.69; H, 4.68; Mo, 10.70; S, 32.61; P, 3.55; N, 1.39.

Bis(tetraphenylphospbonium) *cis-syn*-Bis(η^2-perthiocarbonato)bis(μ-sulfido)bis(tbiomolybdate(V)) Dimethylformamide Hemisolvate, $[Ph_4P]_2[syn\text{-}cis\text{-}Mo_2(S)_2(\mu\text{-}S)_2(\eta^2\text{-}CS_4)_2]\cdot{}^1/_2DMF$ (III). An amount of $[Ph_4P]_2[syn\text{-}Mo_2(S)_2(\mu\text{-}S)_2(\eta^2\text{-}S_4)(\eta^2\text{-}S_2)]$[10] (0.2 g, 0.16 mmol) was dissolved in 40 mL of DMF. To this solution was added 40 mL of CS_2, and a bright red color developed. Diethyl ether was then added to incipient crystallization. After the mixture was allowed to stand for 2 h, red needles formed and were isolated by filtration. The weight of the product after washing with three 30-mL portions of diethyl ether and air-drying was 0.16 g (76% yield). Anal. Calcd for $C_{51.5}H_{43.5}P_2Mo_2S_{12}N_{0.5}O_{0.5}$ (fw = 1314.5): C, 47.00; H, 3.33; Mo, 14.58; S, 29.24. Found: C, 46.25; H, 3.37; Mo, 14.97; S, 30.12. FT-IR (KBr pellet; cm^{-1}): ν(Mo–S_b) 464 (w), ν(C=S) 982 (s). UV–vis (DMF solution, 10^{-3} M; nm): 314 (sh), 365 (sh), 470 (sh), 610 (sh).

Bis(tetraphenylphosphonium) *syn*-Bis(η^2-trithiocarbonato)bis(μ-sulfido)bis(thiomolybdate(V)), $[Ph_4P]_2[syn\text{-}Mo_2(S)_2(\mu\text{-}S)_2(\eta^2\text{-}CS_3)_2]$ (IV). An amount of $[Ph_4P]_2[Mo_2S_6]$[11] (2.00 g, 1.88 mmol) was dissolved in 50 mL of DMF, and to the solution was added 3 mL of CS_2 with stirring. The reaction mixture was stirred for 20 h at ambient temperature and then filtered. To the filtrate was added a layer of ether (100 mL) without disturbing the interface, and the mixture was allowed to diffuse for 5 days. At this time, the red, rod-shaped crystals that formed were isolated and washed with diethyl ether. The yield after drying was 1.6 g (74%). Anal. Calcd for $C_{50}H_{40}P_2S_{10}Mo_2$ (fw = 1214): C, 49.42; H, 3.29; P, 5.11; Mo, 15.82; S, 26.36. Found: C, 49.85; H, 3.58; P, 4.79; Mo, 15.65; S, 26.09. FT-IR (KBr pellet; cm^{-1}): ν(Mo–S_b) 460 (w), ν(C=S) 1052 (s). UV–vis (DMF solution, 10^{-3} M; nm): 344, 444 (sh).

Bis(tetraethylammonium) *syn*-(η^2-Perthiocarbonato)(η^2-trithiocarbonato)bis(μ-sulfido)bis(oxomolybdate(V)), $[Et_4N]_2[syn\text{-}Mo_2(O)_2(\mu\text{-}S)_2(\eta^2\text{-}CS_4)(\eta^2\text{-}CS_3)]$ (V). An amount of $[Et_4N]_2[Mo_2(O)_2(\mu\text{-}S)_2(\eta^2\text{-}S_4)(\eta^2\text{-}S_2)]$[10] (2 g, 2.7 mmol) was dissolved in 100 mL of DMF in air. To this solution was added with stirring an excess of CS_2 (3 mL), and the reaction mixture was stirred for 2 h. To the bright red solution, after filtration, was added 400 mL of ether, and the solution was allowed to stand. The red oil that formed after $^1/_2$ h eventually crystallized after standing at ambient temperature for ca. 10 days. The yield of the red crystals after washing with ether and drying was 2.1 g (97.6%). Anal. Calcd for $C_{18}H_{40}O_2N_2S_9Mo_2$ (fw = 794): C, 27.2; H, 5.04; N, 3.53. Found: C, 27.0; H, 5.01; N, 3.54. FT-IR (KBr pellet; cm^{-1}): ν(Mo–S_b) 469 (w), ν(Mo=O) 950 (s), ν(C=S, CS_4) 982 (s), ν(C=S, CS_3) 1054 (s). UV–vis (DMF solution, 10^{-3} M; nm): 374 (sh), 460.

Bis(tetraphenylphosphonium) *syn*-(η^2-Perthiocarbonato)(η^2-trithiocarbonato)bis(μ-sulfido)bis(oxomolybdate(V)), $[Ph_4P]_2[syn\text{-}Mo_2(O)_2(\mu\text{-}S)_2(\eta^2\text{-}CS_4)(\eta^2\text{-}CS_3)]$. To a clear orange solution of $[Ph_4P]_2[Mo_2(O)_2(\mu\text{-}S)_2(S_4)(S)]$[2], in CH_3CN, was added an excess of CS_2. An amount of diethyl ether was added until the two phases became one, and the solution was stirred for 12 h. The yellow solution was filtered and upon addition of ether deposited the microcrystalline product in good yield. Anal. Calcd for $C_{50}H_{40}P_2O_2S_9Mo_2$ (fw = 1215.2): C, 49.4; H, 3.32. Found: C, 48.7; H, 3.05. FT-IR (KBr pellet; cm^{-1}): ν(Mo–S_b) 466 (w), ν(Mo=O) 953 (s), ν(C=S, CS_4) 979 (s), ν(C=S, CS_3) 1051 (s). UV–vis (DMF solution, 10^{-3} M; nm): 374 (sh), 460. FAB mass spectrum (in 3-nitrobenzyl alcohol): m/z 876 ($P\text{–}Ph_4P^+ = P^-$).

Bis(tetraethylammonium) *syn*-(η^2-Trithiocarbonato)(η^2-tetrasulfido)bis(μ-sulfido)bis(oxomolybdate(V)), $[Et_4N]_2[syn\text{-}Mo_2(O)_2(\mu\text{-}S)_2(\eta^2\text{-}S_4)(\eta^2\text{-}CS_3)]$ (VI). This complex was obtained by a published[3] procedure.

Bis(tetraethylammonium) *syn*-(η^2-Trithiocarbonato)(η^2-disulfido)bis(μ-sulfido)bis(thiomolybdate(V)), $[Et_4N]_2[syn\text{-}Mo_2(O)_2(\mu\text{-}S)_2(\eta^2\text{-}S_2)(\eta^2\text{-}CS_3)]$ (VII). To a suspension of $Mo_2O_2S_2(S_2)(DMF)_3$[3,12] (0.5 g, 0.87 mmol) in 20 mL of H_2O was added an excess of $Et_4NCl\cdot xH_2O$ (0.5 g). While the mixture was stirred, an excess of Na_2CS_3(aq) (0.5 mL, 40% solution, from Strem) was added. The resulting suspension was stirred for about 2 h and then was filtered. The solid was washed with H_2O, isopropyl alcohol, ether, CS_2, and ether in this order. The solid was next extracted in CH_3CN, and to the clear orange solution was added ether to incipient crystallization. The product was isolated in 70% yield. Anal. Calcd for $C_{18}H_{40}N_2S_8OMo$ (fw = 653): C, 33.10; H, 6.17; N, 4.29; Mo, 14.69; S, 39.28. Found: C, 31.92; H, 6.39; N, 4.18; Mo, 15.67; S, 41.91. FT-IR (KBr pellet; cm^{-1}): ν(Mo=O) 952 (vs), ν(Mo–S_b) 479 (w), ν(Mo–η^2-S_2) 522 (mw), ν(Mo–η^2-CS_3) 1051 (m). ^{13}C NMR (DMSO-d_6; ppm): δ = 255 ppm (C=S).

Bis(tetraethylammonium) *syn*-Bis(η^2-trithiocarbonato)bis(μ-sulfido)bis(oxomolybdate(V)), $[Et_4N]_2[syn\text{-}Mo_2(O)_2(\mu\text{-}S)_2(\eta^2\text{-}CS_3)_2]$ (VIII). Method A. To a clear yellow solution of $[Mo_2O_2S_2(DMF)_6][I]_2$[12] (1 g, 1.02 mmol) in 50 mL of H_2O was added a 40% aqueous solution of Na_2CS_3 (0.8 mL, 2.04 mmol, Strem) with stirring. The solution became cloudy, but very soon it turned to a clear orange color. To this orange solution was added $Et_4NCl\cdot xH_2O$ (0.34 g, 2.04 mmol) in 20 mL of H_2O, and a yellow suspension immediately formed. The solid was filtered off and washed in order with H_2O, EtOH, and Et_2O. The yellow solid was recrystallized from CH_3CN/ether. An orange crystalline solid was obtained in good yield. Anal. Calcd for $C_{18}H_{40}O_2N_2S_8Mo_2$ (fw = 764.9): C, 28.26; H, 5.27; N, 3.66. Found: C, 28.64; H, 5.48; N, 3.53. FT-IR (KBr pellet; cm^{-1}): ν(Mo–S_b) 470 (w), ν(Mo=O) 950 (s) and 938 (mw),

(10) Draganjac, M.; Simhon, E.; Chan, L. T.; Kanatzidis, M.; Baenziger, N. C.; Coucouvanis, D. *Inorg. Chem.* **1982**, *21*, 3321.

(11) Hadjikyriacou, A. I.; Coucouvanis, D. *Inorg. Chem.* **1987**, *26*, 2400.

(12) Coucouvanis, D.; Toupadakis, A.; Hadjikyriacou, A. I. *Inorg. Chem.* **1988**, *27*, 3272.

Table I. Summary of Crystal Data, Intensity Collection, and Structure Refinement for *trans*-$[Ph_4P]_2[Mo(S)(CS_4)_2]\cdot DMF$ (I), *cis*-$[Ph_4P][Et_4N][Mo(S)(CS_4)_2]$ (II), *cis-syn*-$[Ph_4P]_2[Mo_2(S)_2(\mu\text{-}S)_2(CS_4)_2]\cdot{}^1/_2DMF$ (III), *syn*-$[Ph_4P]_2[Mo_2(S)_2(\mu\text{-}S)_2(CS_3)_2]$ (IV), and *syn*-$[Et_4N]_2[Mo_2(O)_2(\mu\text{-}S)_2(CS_4)(CS_3)]$ (V)

	I	II	III	IV	V
formula	$C_{53}H_{47}P_2MoS_9NO$	$C_{34}H_{40}PNMoS_9$	$C_{51.5}H_{43.5}P_2Mo_2S_{12}N_{0.5}O_{0.5}$	$C_{50}H_{40}P_2S_{10}Mo_2$	$C_{18}H_{40}N_2O_2S_9Mo_2$
MW	1098.5	878.2	1316.0	1214.9	796.4
a, Å	19.769 (7)	8.024 (2)	10.748 (3)	10.655 (3)	13.005 (4)
b, Å	13.345 (5)	18.371 (5)	12.262 (4)	13.720 (5)	31.879 (8)
c, Å	21.647 (8)	27.183 (5)	22.377 (7)	19.764 (5)	15.540 (4)
α, deg	90.00	90.00	75.66 (3)	90.90 (3)	90.00
β, deg	111.21 (3)	90.00	87.70 (2)	102.43 (2)	90.00
γ, deg	90.00	90.00	80.49 (3)	112.08 (2)	90.00
V, Å^3; Z	5324: 4	4007; 4	2818; 2	2600; 2	6422; 8
d_{calcd}, g/cm^3	1.42	1.453	1.509	1.552	1.647
d_{obsd},[a] g/cm^3	1.45 (2)[a]	1.45 (2)[a]	1.52 (2)[d]	1.55 (2)[d]	1.65 (2)[d]
space group	$P2_1/a$	*Pbcm*	$P\bar{1}$	$P\bar{1}$	*Pnca*
cryst dimens, mm	0.02 × 0.24 × 0.13	0.13 × 0.42 × 0.44	0.08 × 0.40 × 0.28	0.20 × 0.25 × 0.40	0.29 × 0.27 × 0.27
μ, cm^{-1}	6.7	8.9	9.5	9.2	13.1
radiation	Mo Kα[b]	Mo Kα[b]	Mo Kα[b]	Mo Kα[b]	Mo Kα[b]
2θ max, deg	40	40	40	45	45
no of data used, $F_o^2 > 3\sigma(F_o^2)$	2622	1424	2648	3998	2160
no. of params	339	148	371	578	256
R[c]	0.046	0.059	0.064	0.031	0.075
R_w[d]	0.055	0.081	0.075	0.030	0.078

[a] Obtained by flotation in a CCl_4/pentane mixture. [b] λ = 0.71069 Å. [c] $R = \sum||F_o| - |F_c||/\sum|F_o|$. [d] $R_w = [\sum w(|F_o| - |F_c|)^2/\sum w|F_o|^2]^{1/2}$. [e] Obtained by flotation in a CBr_4/pentane mixture.

ν(C=S) 1043 (vs). UV–vis (DMF solution, 10^{-3} M; nm): 380 (sh), 322, 280, 262. FAB mass spectrum (in 3-nitrobenzyl alcohol): m/z 634 (P – Et_4N^+). ^{13}C NMR (DMSO-d_6; ppm): δ = 252.97 (C=S), δ = 7.01, 51.50 [Et_4N^+].

Method B. $[Et_4N]_2[Mo_2(O)_2(\mu\text{-}S)_2(\eta^2\text{-}CS_4)(\eta^2\text{-}CS_3)]$ (V) (1 g, 1.26 mmol) and Ph_3P (0.33 g, 1.25 mmol) were dissolved in 70 mL of DMF, and the solution was stirred for 2 h at ambient temperature. Upon addition of 150 mL of diethyl ether, an orange-red oil deposited on the wall of the container and crystallized upon standing for several days. The yellow-orange crystals were isolated, washed with diethyl ether, and air-dried. The yield after drying was 0.6 g (62%). Anal. Calcd for $C_{18}H_{40}N_2S_8O_2Mo_2$ (fw = 764.9): C, 28.26; H, 5.27; N, 3.66; S, 33.5; Mo, 25.1. Found: C, 28.6; H, 5.48; N, 3.53; S, 32.8; Mo, 24.5. FT-IR (KBr pellet; cm^{-1}): ν(Mo–S_b) 470 (w), ν(C=S) 1043 (s), ν(Mo=O) 950 (s), 938 (m). FAB mass spectrum (in 3-nitrobenzyl alcohol): m/z 634 (P – Et_4N^+). ^{13}C NMR (DMSO-d_6; ppm): δ = 252.97 (C=S), δ = 7.01, 51.50 (Et_4N^+).

Physical Methods. Visible and ultraviolet spectra were obtained on a Cary Model 219 spectrophotometer. Infrared spectra were recorded on a Nicolet 60 SX FT-IR spectrometer at a resolution of 4 cm^{-1} in CsI disks. ^{13}C NMR spectra were obtained on a Bruker 300-MHz pulse FT NMR spectrometer with Me_4Si as internal standard. Chemical shifts are reported in parts per million (ppm).

X-ray Diffraction Measurements. (a) Collection of Data. Single crystals of $[Ph_4P]_2[trans\text{-}(S)Mo(\eta^2\text{-}CS_4)_2]\cdot DMF$ (I), $[Ph_4P][Et_4N][cis\text{-}(S)Mo(\eta^2\text{-}CS_4)_2]$ (II), $[Ph_4P]_2[syn\text{-}cis\text{-}Mo_2(S)_2(\mu\text{-}S)_2(\eta^2\text{-}CS_4)_2]\cdot{}^1/_2DMF$ (III), $[Ph_4P]_2[syn\text{-}Mo_2(S)_2(\mu\text{-}S)_2(\eta^2\text{-}CS_3)_2]$ (IV), and $[Et_4N]_2[Mo_2(O)_2(\mu\text{-}S)_2(\eta^2\text{-}CS_4)(\eta^2\text{-}CS_3)]$ (V) were obtained by the slow diffusion of diethyl ether into DMF solutions of the complexes.

A single crystal for each complex was carefully chosen and mounted in a thin-walled, sealed capillary tube. Diffraction data for I–III were obtained on a Picker-Nuclear four-circle diffractometer equipped with a scintillation counter and a pulse height analyzer and automated by a DEC PDP8-I computer and disk with FACS-I DOS software. Intensity data for IV and V were collected on a Nicolet P3/F four-circle, computer-controlled diffractometer at ambient temperature. Graphite-monochromatized Mo Kα radiation ($2\theta_{max}$ = 12.50°) was used for data collection and cell dimension measurements (Kα, λ = 0.7107 Å).

Intensity data for all crystals were obtained using a θ–2θ step scan technique. Throughout the data collection, three standard reflections were monitored every 100 reflections to verify crystal and instrumental stability. No crystal decay was observed for any of the crystals. Accurate cell parameters were obtained from a least-squares fit of the angular settings (2θ, ω, ϕ, χ) of 25 machine-centered reflections with 2θ values between 20 and 30°. Details concerning crystal characteristics and X-ray diffraction methodology are shown in Table I.

The protocol followed for the reduction of data and for the structure solutions and refinements has been described in detail previously.[13]

Due to the small μ values (Table I) and the small size of the crystals, no absorption corrections were applied to any of the data sets.

(b) Determination of Structures. Three-dimensional Patterson synthesis maps along with the direct-methods routine SOLV of the SHELXTL 84 package of crystallographic programs or MULTAN[14] (for I–III) were employed to locate Mo or S atoms. Subsequent difference Fourier maps were used to locate all other non-hydrogen atoms in the asymmetric units.

$[Ph_4P]_2[trans\text{-}(S)Mo(\eta^2\text{-}CS_4)_2]\cdot DMF$ (I). A three-dimensional Patterson synthesis map was used to locate the positions of the molybdenum atom and the five sulfur atoms closest to the metal. All other non-hydrogen atoms were located on subsequent Fourier syntheses following least-squares refinements of the atomic input coordinates. The refinement of all atoms with isotropic temperature factors in the monoclinic nonstandard space group $P2_1/a$ gave a conventional R value of 0.069. Further refinement of the structure with anisotropic temperature factors for the atoms of the anion and the two phosphorus atoms of the cations gave a conventional R value of 0.055. Hydrogen atoms were included in the structure factor calculation at their calculated positions (0.95 Å from the carbon atoms) but were not refined. The final R value was 0.046; the weighted R was 0.055. During the last cycle of refinement, all parameter shifts were less than 10% of their esd's.

$[Ph_4P][Et_4N][cis\text{-}(S)Mo(\eta^2\text{-}CS_4)_2]$ (II). The atomic positions of the molybdenum and three of the sulfur atoms were located by direct methods using the program MULTAN.[14] All other nonhydrogen atoms were located on subsequent Fourier syntheses following least-squares refinements of the atomic input coordinates. The refinement of all atoms with isotropic temperature factors in the orthorhombic space group *Pbcm* gave a conventional R value of 0.101. The centrosymmetric space group was chosen (rather than the acentric $Pbc2_1$) on the basis of nearly unequivocal intensity statistics. The successful refinement of the structure further justified this choice. Further refinement of the structure with anisotropic temperature factors for the atoms of the anion gave a conventional R value of 0.064. Hydrogen atoms were included in the structure factor calculation at their calculated positions (0.95 Å from the carbon atoms) but were not refined. The final R value was 0.059; the weighted R was 0.081. During the last cycle of refinement, all parameter shifts were less than 10% of their esd's.

$[Ph_4P]_2[syn\text{-}cis\text{-}Mo_2(S)_2(\mu\text{-}S)_2(\eta^2\text{-}CS_4)_2]\cdot{}^1/_2DMF$ (III). The atomic coordinates of the two molybdenum atoms and the eight metal-bound sulfur atoms, as well as the cations, were taken directly from the final least-squares refinement of the isomorphous $(Ph_4P)_2[(Mo_2S_{10})_{0.72}(Mo_2S_{12})_{0.28}]\cdot{}^1/_2DMF$ complex.[10] The other atoms of the anion and the DMF of solvation were located on subsequent Fourier syntheses following least-squares refinement of the input atomic coordinates. Isotropic refinement of the carbon atoms in the cations and anisotropic refinement of all atoms in the anion and of the two phosphorus atoms in the cations converged to a conventional R value of 0.087. Inclusion of the H atoms

(13) Al-Ahmad, S. A.; Salifoglou, A.; Kanatzidis, M. G.; Dunham, W. R.; Coucouvanis, D. *Inorg. Chem.* **1990**, *29*, 927.

(14) Main, P.; Woolfson, M. M.; Germain, G. MULTAN: A Computer Program for the Automatic Solution of Crystal Structures. University of York, York, England.

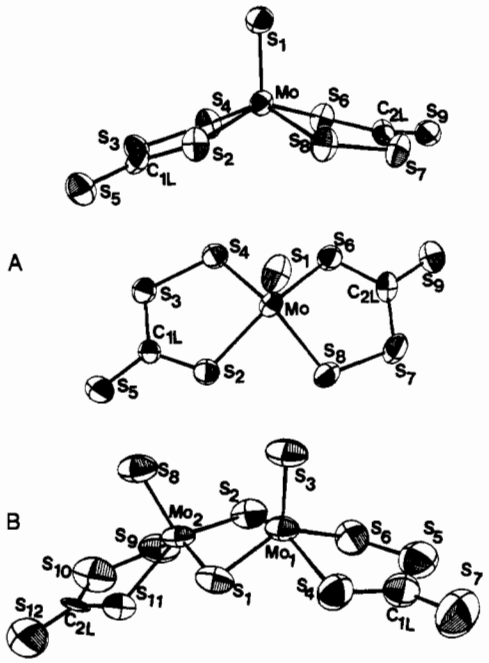

Figure 1. Structure and labeling of the anions in (A) $[Ph_4P]_2[trans\text{-}(S)Mo(\eta^2\text{-}CS_4)_2]\cdot DMF$ (I) (two views) and (B) $[Ph_4P]_2[syn\text{-}cis\text{-}Mo_2(S)_2(\mu\text{-}S)_2(\eta^2\text{-}CS_4)_2]\cdot{}^1/_2DMF$ (III). Thermal ellipsoids as drawn by ORTEP represent the 40% probability surfaces.

as described above for I and II resulted in a final R value of 0.064. The weighted R was 0.075. During the last cycle of refinement, all parameter shifts were less than 10% of their esd's.

$[Ph_4P]_2[syn\text{-}Mo_2(S)_2(\mu\text{-}S)_2(\eta^2\text{-}CS_3)_2]$ (IV). The coordinates of the molybdenum and six sulfur atoms were obtained from the direct methods routine TREF of the SHELX-PLUS crystallographic package. These positions were verified also in the Patterson map. Two sulfur and two carbon atoms in the anion were located via successive difference Fourier electron density maps. The refinement of all atoms with isotropic temperature factors in the triclinic space group $P\bar{1}$ gave a conventional R value of 0.081. All non-hydrogen atoms in the unit cell were refined with anisotropic temperature factors to give an R value of 0.041. Finally, the H atoms were included in the structure factor calculation but were not refined. The final R and R_w values were 0.031 and 0.030, respectively.

$[Et_4N]_2[Mo_2(O)_2(\mu\text{-}S)_2(\eta^2\text{-}CS_4)(\eta^2\text{-}CS_3)]$ (V). The structure was solved in the nonstandard space group *Pnca*. The coordinates of the molybdenum and five sulfur atoms were obtained from the direct methods routine TREF of the SHELX-PLUS crystallographic package. These positions were verified also in the Patterson map. The remaining atoms in the asymmetric unit were located in subsequent difference Fourier electron density maps. The last atoms to be located were the carbon atoms of one full cation and of the two disordered half-occupancy cations. The two nitrogen atoms of the half-occupancy, disordered Et_4N^+ cations were located on special positions at (0.25, 0.25, 0.30) and (0.25, 0.50, 0.30). The refinement of all atoms with isotropic temperature factors gave a conventional R value of 0.127. Assignment of anisotropic temperature factors to all atoms, except for one terminal oxygen atom and the carbon atoms of the disordered cations, and subsequent refinement calculations resulted in a final R value of 0.092. Finally, the H atoms were included in the structure factor calculation but were not refined. The final R and R_w values were 0.075 and 0.077, respectively.

(c) Crystallographic Results. The final atomic positional parameters for $[Ph_4P]_2[trans\text{-}(S)Mo(\eta^2\text{-}CS_4)_2\cdot DMF$ (I), $[Ph_4P][Et_4N][cis\text{-}(S)Mo(\eta^2\text{-}CS_4)_2]$ (II), $[Ph_4P]_2[syn\text{-}cis\text{-}Mo_2(S)_2(\mu\text{-}S)_2(\eta^2\text{-}CS_4)_2]\cdot{}^1/_2DMF$ (III), $[Ph_4P]_2[syn\text{-}Mo_2(S)_2(\mu\text{-}S)_2(\eta^2\text{-}CS_3)_2]$ (IV), and $[Et_4N]_2[Mo_2(O)_2(\mu\text{-}S)_2(\eta^2\text{-}CS_4)(\eta^2\text{-}CS_3)]$ (V) with standard deviations are shown in Tables II–VI. Intermolecular distances and angles are given in Table VII. The numbering scheme for the anions in I–V are shown in Figures 1–4.

Results and Discussion

Synthesis. The generation of the perthiocarbonate anion, CS_4^{2-}, generally is accomplished by the addition of a polysulfide or disulfide dianion to CS_2. The associated counterions include Na^+, K^+, Cs^+, Sn^{2+}, and NH_4^+.[15] The $[M(CS_4)_2]^{2-}$ complexes can be generated from the $[M(CS_3)_2]^{2-}$ complexes (M = Ni, Pt) by either I_2 oxidation or sulfur addition reactions.[16]

Addition of CS_2 to DMF solutions of $[Ph_4P]_2[(S)Mo(\eta^2\text{-}S_4)_2]$ and $[Ph_4P]_2[syn\text{-}Mo_2(S)_2(\mu\text{-}S)_2(\eta^2\text{-}S_4)(\eta^2\text{-}S_2)]$ results in the formation of the perthiocarbonate derivative complexes I–III. The mechanisms by which the CS_4^{2-} ligands in either I, II, or III are obtained very likely involve CS_2 insertion into either the Mo=S or Mo—η^2-S_2 bonds in the $[(S)Mo(\eta^2\text{-}S_4)_2]^{2-}$ and $[Mo_2(S)_2(\mu\text{-}S)_2(\eta^2\text{-}S_4)(\eta^2\text{-}S_2)]^{2-}$ complexes. The isolation of both geometrical isomers I and II undoubtedly is due to solubility differences of the two isomers in different solvents and with different counterions. The superior reactivity of either the Mo=S or the Mo-η^2-S_2 groups toward electrophiles, by comparison to the Mo-η^2-S_4 group, is aptly demonstrated in the relative reactivities of the $[(S_4)_2Mo^{IV}{=}O]^{2-}$ and $[(S_4)_2Mo^{IV}{=}S]^{2-}$ complexes toward CS_2. The latter readily reacts with CS_2 to give both *cis*- and *trans*-$[(CS_4)_2Mo^{IV}{=}S]^{2-}$ complexes.[4,7] In contrast, the $[(S_4)_2Mo^{IV}{=}O]^{2-}$ complex is unreactive toward CS_2, unless activated by Ph_3P.[8] Presumably, Ph_3P "activation" involves the generation of reactive η^2-S_2 or Mo=S units from the Mo-coordinated η^2-S_4 ligands. These observations suggest either that the lack of reactivity of the $[(S_4)_2Mo^{IV}{=}O]^{2-}$ complex toward CS_2 is due to the absence of a reactive Mo=S functional group or that the Mo=O group in $[(S_4)_2Mo^{IV}{=}O]^{2-}$ prevents the dissociation of S_2 from the Mo-η^2-S_4 units and for-

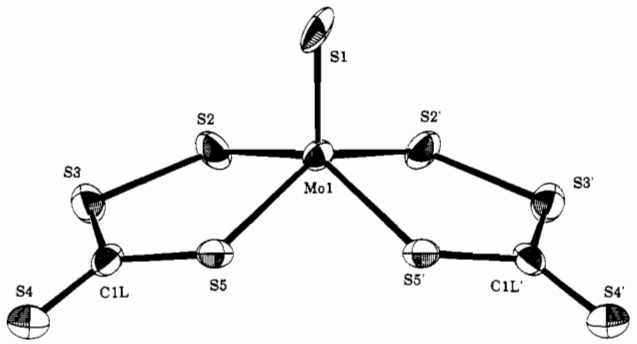

Figure 2. Structure and labeling of the anion in $[Ph_4P][Et_4N][cis\text{-}(S)\text{-}Mo(\eta^2\text{-}CS_4)_2]$ (II). Thermal ellipsoids as drawn by ORTEP represent the 40% probability surfaces.

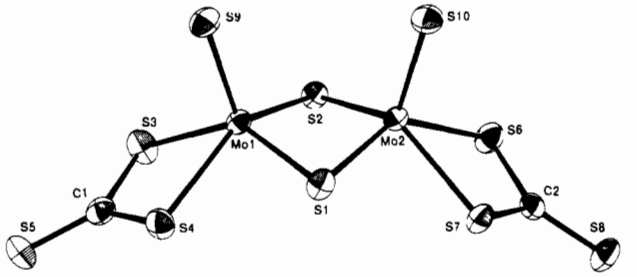

Figure 3. Structure and labeling of the anion in $[Ph_4P]_2[syn\text{-}Mo_2(S)_2\text{-}(\mu\text{-}S)_2(\eta^2\text{-}CS_3)_2]$ (IV). Thermal ellipsoids as drawn by ORTEP represent the 40% probability surfaces.

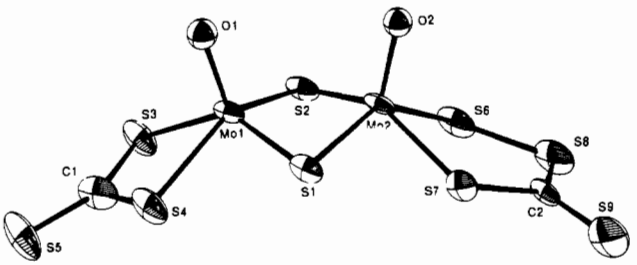

Figure 4. Structure and labeling of the anion in $[Et_4N]_2[Mo_2(O)_2(\mu\text{-}S)_2(\eta^2\text{-}CS_4)(\eta^2\text{-}CS_3)]$ (V). Thermal ellipsoids as drawn by ORTEP represent the 40% probability surfaces.

(15) Gattow, G.; Behrendt, W. *Topics in Sulfur Chemistry*; Georg Thieme Publishers: Stuttgart, Germany, 1977; Vol. 2, p 173.

(16) Coucouvanis, D.; Fackler, J. P., Jr. *J. Am. Chem. Soc.* **1967**, *89*, 1346.

Table II. Positional and Anisotropic[a] and Isotropic[b] Thermal Parameters with Their Standard Deviations for *trans*-$[Ph_4P]_2[Mo(S)(CS_4)_2]\cdot DMF$ (I)

atom	x	y	z	B_{11}[a] (B[b])
Mo	0.45468 (6)	−0.00439 (8)	0.25901 (5)	3.48 (5)
S1	0.4938 (2)	0.0439 (2)	0.3594 (2)	6.8 (2)
S2	0.4999 (2)	0.1000 (2)	0.1973 (2)	3.5 (2)
S3	0.4237 (2)	0.2107 (2)	0.1485 (2)	3.7 (2)
S4	0.2720 (2)	0.2456 (3)	0.1154 (2)	3.7 (2)
S5	0.3403 (2)	0.0747 (2)	0.2043 (2)	3.6 (2)
S6	0.5431 (2)	−0.1151 (2)	0.2463 (2)	3.6 (2)
S7	0.5895 (2)	−0.3276 (3)	0.2632 (2)	5.6 (2)
S8	0.4433 (2)	−0.2776 (2)	0.2547 (2)	5.8 (2)
S9	0.3820 (2)	−0.1463 (2)	0.2467 (2)	4.0 (2)
C1L	0.3430 (6)	0.1767 (8)	0.1556 (5)	2.8 (6)
C2L	0.4734 (6)	0.2411 (8)	0.7442 (5)	4.4 (7)
P1	0.0574 (2)	0.2012 (2)	−0.0064 (2)	3.7 (2)
P2	0.1540 (2)	−0.0186 (2)	0.4703 (1)	4.3 (2)
C1	−0.0396 (6)	0.2129 (8)	−0.0374 (5)	2.8 (2)
C2	−0.0816 (7)	0.1762 (9)	−0.0027 (6)	3.7 (3)
C3	−0.1560 (7)	0.1866 (9)	−0.0283 (6)	4.3 (3)
C4	−0.1887 (7)	0.231 (1)	−0.0877 (6)	4.4 (3)
C5	−0.1484 (7)	0.2681 (9)	−0.1233 (6)	4.5 (3)
C6	−0.0734 (6)	0.2613 (9)	−0.0975 (6)	3.3 (3)
C7	0.0927 (6)	0.3240 (9)	−0.0100 (6)	3.3 (3)
C8	0.0785 (8)	0.400 (1)	0.0269 (7)	6.8 (4)
C9	0.1019 (8)	0.498 (1)	0.0209 (8)	7.5 (4)
C10	−0.1364 (7)	0.482 (1)	0.0214 (7)	5.7 (3)
C11	0.1488 (8)	0.444 (1)	−0.0585 (8)	6.8 (4)
C12	0.1252 (7)	0.346 (1)	−0.0535 (7)	5.1 (3)
C13	0.0846 (6)	0.1187 (8)	−0.0586 (5)	2.6 (2)
C14	0.1580 (7)	0.1032 (9)	−0.0450 (6)	4.0 (3)
C15	0.1777 (7)	0.037 (1)	−0.0852 (7)	5.1 (3)
C16	0.1264 (6)	−0.0130 (9)	−0.1363 (6)	3.7 (3)
C17	0.543 (6)	0.0049 (9)	−0.1492 (5)	3.3 (2)
C18	0.0336 (6)	0.0702 (8)	−0.1106 (6)	3.3 (3)
C19	0.0897 (6)	0.1530 (8)	0.0764 (5)	2.9 (2)
C20	0.1232 (6)	0.0599 (9)	0.0891 (6)	3.8 (3)
C21	0.1484 (6)	0.0206 (9)	0.1532 (6)	4.3 (3)
C22	0.1388 (7)	0.077 (1)	0.2043 (6)	4.5 (3)
C23	0.1059 (7)	0.165 (1)	0.1912 (6)	4.7 (3)
C24	0.0816 (6)	0.2052 (9)	0.1278 (6)	3.9 (3)
C25	0.0833 (6)	0.0445 (8)	0.4049 (5)	2.7 (2)
C26	0.0922 (7)	0.1458 (9)	0.3905 (6)	3.9 (3)
C27	0.0381 (7)	0.192 (1)	0.3413 (6)	4.5 (3)
C28	−0.0246 (7)	0.146 (1)	0.3077 (6)	4.2 (3)
C29	−0.0364 (7)	0.049 (1)	0.3206 (6)	4.6 (3)
C30	0.0186 (6)	−0.0032 (9)	0.3697 (5)	3.4 (2)
C31	0.2336 (6)	−0.0372 (8)	0.4490 (6)	3.2 (3)
C32	0.2863 (7)	−0.1012 (9)	0.4872 (6)	4.0 (3)
C33	0.3488 (7)	−0.115 (1)	0.4727 (7)	5.0 (3)
C34	0.3541 (7)	−0.069 (1)	0.4187 (7)	5.1 (3)
C35	0.3016 (7)	−0.009 (1)	0.3799 (6)	5.3 (3)
C36	0.2404 (6)	0.012 (1)	0.3943 (6)	4.4 (3)
C37	0.1206 (6)	−0.1365 (8)	0.4843 (5)	2.9 (2)
C38	0.0985 (6)	−0.1535 (9)	0.5375 (6)	3.6 (3)
C39	0.0704 (7)	−0.246 (1)	0.5434 (6)	5.3 (3)
C40	0.0617 (7)	−0.3198 (9)	0.4983 (6)	4.2 (3)
C41	0.0840 (7)	−0.305 (1)	0.4466 (6)	4.7 (3)
C42	0.1141 (7)	−0.2138 (9)	0.4392 (6)	4.4 (3)
C43	0.1751 (6)	0.0594 (8)	0.5418 (5)	2.7 (2)
C44	0.2464 (7)	0.0815 (9)	0.5808 (6)	3.9 (3)
C45	0.2595 (7)	0.144 (1)	0.6357 (7)	5.0 (3)
C46	0.2052 (7)	0.185 (1)	0.6509 (6)	4.7 (3)
C47	0.1344 (7)	0.163 (1)	0.6121 (6)	4.6 (3)
C48	0.1180 (7)	0.1031 (9)	0.5558 (6)	3.8 (3)
N	0.7234 (6)	0.1314 (8)	0.2823 (6)	5.3 (3)
C(1)	0.7096 (9)	0.063 (1)	0.2295 (8)	7.9 (4)
C(2)	0.7777 (9)	0.209 (1)	0.2906 (8)	7.6 (4)
C(3)	0.6859 (8)	0.129 (1)	0.3232 (8)	5.8 (4)
O	0.6972 (6)	0.1878 (8)	0.3680 (5)	7.9 (3)

[a] The thermal parameters are in units of Å^2. The temperature factor for the anisotropic case has the form $T = \sum((1/4)B_{ij}H_iH_{j\alpha}{}^*{}_i a^*{}_j)$ where H is the Miller index, a^* is the reciprocal cell length, and i and j are cycled 1–3. [b] For the isotropic temperature factors, $T = -B((\sin\theta)/\lambda)^2$. In this table isotropic temperature factors are reported for the cation carbon atoms (C(1) and below) and for the atoms in the DMF molecule of solvation.

Table III. Positional and Anisotropic[a] and Isotropic[b] Thermal Parameters with Their Standard Deviations for *cis*-$[Ph_4P][Et_4N][MoS(CS_4)_2]$ (II)

atom	x	y	z	B_{11}[a] (B[b])
Mo	0.8172 (1)	0.09172 (6)	0.750	4.51 (7)
S1	1.0815 (5)	0.1367 (3)	0.750	7.1 (3)
S2	0.6513 (4)	0.1514 (1)	0.8071 (1)	8.6 (2)
S3	0.6520 (4)	0.0976 (2)	0.8754 (1)	6.8 (2)
S4	0.7310 (4)	−0.0460 (2)	0.5917 (1)	7.4 (2)
S5	0.8146 (3)	0.5072 (1)	0.3064 (1)	4.3 (1)
C1L	0.737 (1)	0.0126 (5)	0.6348 (4)	3.8 (4)
P	0.4666 (4)	0.250	0.500	4.5 (3)
N	0.684 (1)	0.1014 (7)	0.250	4.9 (3)
C1	0.332 (1)	0.2890 (5)	0.4548 (3)	3.4 (2)
C2	0.344 (1)	0.2707 (5)	0.4054 (4)	4.9 (2)
C3	0.230 (1)	0.2997 (6)	0.3722 (4)	5.8 (2)
C4	0.109 (1)	0.3458 (6)	0.3868 (4)	5.5 (2)
C5	0.096 (1)	0.3640 (6)	0.4371 (4)	5.2 (2)
C6	0.208 (1)	0.3356 (6)	0.4698 (4)	4.8 (2)
C7	0.602 (1)	0.1826 (5)	0.4738 (3)	3.6 (2)
C8	0.594 (1)	0.1099 (6)	0.4885 (4)	5.1 (2)
C9	0.715 (1)	0.0626 (7)	0.4711 (4)	6.5 (3)
C10	0.837 (2)	0.0846 (7)	0.4416 (5)	7.3 (3)
C11	0.850 (2)	0.1566 (7)	0.4283 (5)	7.2 (3)
C12	0.730 (1)	0.2060 (6)	0.4447 (4)	5.9 (3)
C1E	0.621 (4)	0.086 (2)	0.184 (1)	8.5 (7)
C1E′	0.624 (4)	0.045 (2)	0.225 (1)	9.7 (8)
C2E	0.695 (2)	0.019 (1)	0.1733 (8)	13.1 (6)
C3E	0.590 (4)	0.170 (1)	0.250	12.2 (7)
C4E	0.422 (3)	0.181 (1)	0.250	8.8 (5)
C5E	0.862 (3)	0.115 (1)	0.250	9.4 (6)
C6E	0.935 (4)	0.173 (2)	0.219 (1)	12.2 (10)

[a] See footnote *a*, Table II. [b] See footnote *b*, Table II. In this table isotropic temperature factors are reported for all the atoms in the Ph_4P^+ and Et_4N^+ cations (P and below).

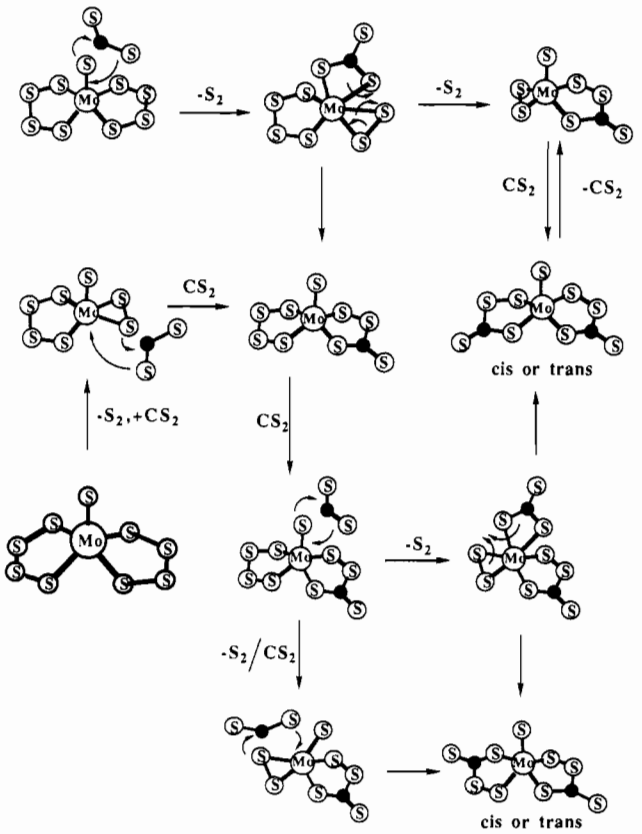

Figure 5. Proposed pathways leading to the synthesis of the $[(S)Mo(\eta^2\text{-}CS_4)_2]^{2-}$ complexes.

mation of a reactive Mo-η^2-S_2 unit.

Proposed pathways that may lead to either *cis*- or *trans*-$[(S)Mo(\eta^2\text{-}CS_4)_2]^{2-}$ complexes in the reactions of CS_2 with $[(S)Mo(\eta^2\text{-}S_4)_2]^{2-}$ are shown in Figure 5. The addition of CS_2

Table IV. Positional and Anisotropic[a] and Isotropic[b] Thermal Parameters with Their Standard Deviations for $[Ph_4P]_2[Mo_2S_4(CS_4)_2]\cdot{}^1/_2DMF$ (III)

atom	x	y	z	B_{11}[a] (B[b])
Mo1	0.4968 (2)	0.6039 (1)	0.23022 (7)	3.83 (9)
Mo2	0.4409 (1)	0.7888 (2)	0.28744 (7)	3.01 (9)
S1	0.3377 (5)	0.6161 (5)	0.1754 (2)	5.1 (3)
S2	0.5611 (6)	0.4096 (5)	0.2843 (3)	7.3 (4)
S3	0.6599 (6)	0.3182 (6)	0.2296 (3)	7.2 (4)
S4	0.7984 (8)	0.3658 (7)	0.1176 (5)	10.1 (6)
S5	0.6771 (5)	0.5624 (5)	0.1667 (3)	5.9 (3)
S6	0.5679 (5)	0.9341 (5)	0.2855 (3)	4.3 (3)
S7	0.5772 (7)	0.1073 (7)	0.3530 (4)	9.3 (5)
S8	0.5377 (7)	0.0810 (6)	0.5871 (3)	9.2 (5)
S9	0.4417 (5)	0.7703 (6)	0.3964 (3)	6.0 (3)
S10	0.2622 (5)	0.8764 (5)	0.2540 (2)	4.4 (3)
S11	0.5723 (5)	0.7759 (5)	0.2044 (2)	4.4 (3)
S12	0.4259 (5)	0.5980 (5)	0.3297 (2)	5.4 (3)
C1L	0.716 (2)	0.417 (2)	0.173 (1)	6.4 (14)
C2L	0.530 (1)	0.996 (2)	0.3509 (8)	3.0 (9)
P1	0.1402 (4)	0.1078 (4)	0.0839 (2)	4.5 (3)
P2	0.0031 (4)	0.2395 (4)	0.5580 (2)	4.1 (3)
C1	0.042 (1)	0.015 (1)	0.1297 (7)	3.0 (3)
C2	0.038 (2)	−0.091 (2)	0.1219 (8)	4.5 (4)
C3	−0.044 (2)	−0.157 (2)	0.1571 (9)	5.2 (5)
C4	−0.118 (2)	−0.120 (2)	0.1970 (9)	5.0 (4)
C5	−0.121 (2)	−0.014 (2)	0.208 (1)	7.3 (6)
C6	−0.037 (2)	0.052 (2)	0.1731 (9)	5.9 (5)
C7	0.046 (2)	0.219 (1)	0.0294 (7)	3.5 (4)
C8	−0.078 (2)	0.212 (2)	0.0196 (8)	4.8 (4)
C9	−0.148 (2)	0.296 (2)	−0.0243 (9)	6.3 (5)
C10	−0.096 (2)	0.386 (2)	−0.0582 (9)	6.4 (5)
C11	0.026 (2)	0.392 (2)	−0.050 (1)	7.4 (6)
C12	0.097 (2)	0.309 (2)	−0.0036 (9)	5.5 (5)
C13	0.214 (2)	0.176 (2)	0.1312 (8)	4.5 (4)
C14	0.145 (2)	0.270 (2)	0.1471 (9)	5.8 (5)
C15	0.195 (2)	0.325 (2)	0.187 (1)	7.7 (6)
C16	0.315 (2)	0.282 (2)	0.208 (1)	7.4 (6)
C17	0.391 (2)	0.192 (2)	0.191 (1)	6.7 (5)
C18	0.337 (2)	0.137 (2)	0.1535 (9)	5.3 (5)
C19	0.251 (2)	0.024 (1)	0.0444 (8)	3.6 (4)
C20	0.258 (2)	0.053 (2)	−0.0203 (8)	4.6 (4)
C21	0.340 (2)	−0.015 (2)	−0.0495 (8)	5.2 (5)
C22	0.418 (2)	−0.109 (2)	−0.0176 (8)	4.7 (4)
C23	0.412 (2)	−0.136 (2)	0.0454 (9)	5.0 (4)
C24	0.328 (2)	−0.072 (2)	0.0774 (8)	4.1 (4)
C25	0.032 (2)	0.311 (1)	0.6143 (7)	3.6 (4)
C26	0.140 (2)	0.359 (2)	0.6143 (8)	4.9 (4)
C27	0.159 (2)	0.414 (2)	0.659 (1)	7.7 (6)
C28	0.067 (2)	0.423 (2)	0.7049 (9)	6.2 (5)
C29	−0.040 (2)	0.373 (2)	0.7057 (9)	5.7 (5)
C30	−0.057 (2)	0.318 (2)	0.6600 (8)	4.6 (4)
C31	−0.007 (2)	0.093 (2)	0.5962 (8)	5.1 (5)
C32	0.099 (3)	0.022 (3)	0.624 (1)	10.2 (8)
C33	0.087 (3)	−0.091 (2)	0.655 (1)	9.8 (7)
C34	−0.018 (2)	−0.127 (2)	0.663 (1)	6.8 (5)
C35	−0.119 (3)	−0.062 (3)	0.637 (1)	10.9 (8)
C36	−0.112 (3)	0.050 (2)	0.603 (1)	9.5 (7)
C37	−0.143 (2)	0.305 (2)	0.5193 (8)	4.2 (4)
C38	−0.187 (2)	0.253 (2)	0.477 (1)	7.3 (6)
C39	−0.298 (2)	0.307 (2)	0.443 (1)	7.3 (6)
C40	−0.362 (2)	0.402 (2)	0.4511 (9)	5.6 (5)
C41	−0.320 (2)	0.453 (2)	0.4913 (9)	5.3 (5)
C42	−0.212 (2)	0.406 (2)	0.5285 (8)	5.2 (5)
C43	0.118 (2)	0.259 (2)	0.4991 (9)	4.9 (4)
C44	0.230 (4)	0.183 (3)	0.506 (2)	14.5 (11)
C45	0.328 (3)	0.206 (3)	0.461 (2)	13.4 (10)
C46	0.305 (2)	0.288 (2)	0.409 (1)	7.2 (6)
C47	0.190 (2)	0.350 (2)	0.401 (1)	6.8 (5)
C48	0.100 (2)	0.331 (2)	0.4456 (9)	5.5 (5)
N	0.500	0.500	0	11.8 (11)
C(1)	0.450 (8)	0.425 (7)	0.048 (4)	8.9 (26)
C(2)	0.436 (7)	0.435 (6)	−0.017 (3)	12.0 (22)
C(3)	0.454 (9)	0.454 (8)	0.057 (5)	11.1 (39)
O	0.3865	0.3534	0.0098	14.5

[a] See footnote *a*, Table II. [b] See footnote *b*, Table II. In this table isotropic temperature factors are reported for the cation carbon atoms (C(1) and below) and for the atoms in the DMF molecule of solvation.

Table V. Fractional Atomic Coordinates and Thermal Parameters for $[Ph_4P]_2[Mo_2(S)_2(\mu\text{-}S)_2(\eta^2\text{-}CS_3)_2]$ (IV)

atom	x	y	z	U[a]
Mo1	−0.0071 (0)	0.3379 (0)	0.2445 (0)	0.047
Mo2	−0.0926 (0)	0.1278 (0)	0.1853 (0)	0.048
S1	−0.0976 (2)	0.4265 (1)	0.3183 (1)	0.077
S2	0.1686 (2)	0.4240 (1)	0.3501 (1)	0.071
S3	0.1134 (2)	0.5713 (1)	0.4415 (1)	0.086
S4	0.0300 (2)	0.4335 (1)	0.1627 (1)	0.077
S5	−0.2303 (1)	0.2104 (1)	0.2146 (1)	0.052
S6	0.1218 (1)	0.2351 (1)	0.2518 (1)	0.063
S7	−0.0078 (2)	−0.0047 (1)	0.2316 (1)	0.068
S8	−0.2895 (2)	−0.0372 (1)	0.1870 (1)	0.068
S9	−0.2187 (2)	−0.2196 (1)	0.2370 (1)	0.092
S10	−0.0863 (2)	0.1365 (1)	0.0805 (1)	0.092
C1	0.0649 (6)	0.4831 (4)	0.3753 (3)	0.061
C2	−0.1759 (6)	−0.0979 (4)	0.2184 (3)	0.061
P1	0.5695 (2)	0.8143 (1)	0.4412 (1)	0.049
C3	0.6234 (6)	0.7086 (4)	0.4263 (3)	0.052
C4	0.5357 (6)	0.6067 (5)	0.4329 (3)	0.069
C5	0.5790 (9)	0.5243 (5)	0.4257 (3)	0.089
C6	0.7076 (9)	0.5435 (6)	0.4134 (3)	0.089
C7	0.7933 (7)	0.6451 (6)	0.4053 (3)	0.078
C8	0.7505 (6)	0.7281 (5)	0.4113 (3)	0.061
C9	0.4256 (6)	0.8106 (4)	0.3742 (3)	0.048
C10	0.3885 (6)	0.8979 (4)	0.3713 (3)	0.059
C11	0.2671 (7)	0.8924 (5)	0.3265 (3)	0.070
C12	0.1813 (7)	0.8014 (6)	0.2848 (3)	0.071
C13	0.2181 (7)	0.7154 (5)	0.2855 (3)	0.068
C14	0.3399 (7)	0.7188 (4)	0.3297 (3)	0.061
C15	0.5169 (6)	0.7974 (4)	0.5223 (3)	0.045
C16	0.6048 (6)	0.7810 (5)	0.5803 (3)	0.072
C17	0.5630 (7)	0.7665 (6)	0.6424 (3)	0.081
C18	0.4377 (7)	0.7662 (5)	0.6472 (3)	0.071
C19	0.3533 (6)	0.7834 (5)	0.5906 (3)	0.068
C20	0.3922 (6)	0.7993 (4)	0.5278 (3)	0.057
C21	0.7120 (6)	0.9386 (4)	0.4465 (3)	0.052
C22	0.7815 (6)	0.9988 (5)	0.5101 (3)	0.060
C23	0.8922 (7)	1.0945 (5)	0.5134 (3)	0.070
C24	0.9346 (7)	1.1278 (5)	0.4538 (4)	0.074
C25	0.8664 (7)	1.0687 (6)	0.3914 (4)	0.077
C26	0.7534 (7)	0.9739 (5)	0.3864 (3)	0.066
P2	−0.4133 (1)	−0.2675 (1)	−0.0515 (1)	0.045
C27	−0.2524 (5)	−0.2603 (5)	0.0028 (3)	0.050
C28	−0.2329 (6)	−0.3529 (5)	0.0180 (3)	0.067
C29	−0.1106 (8)	−0.3469 (7)	0.0630 (4)	0.092
C30	−0.0104 (8)	−0.2498 (8)	0.0926 (3)	0.090
C31	−0.0297 (7)	−0.1602 (6)	0.0775 (3)	0.076
C32	−0.1493 (6)	−0.1629 (5)	0.0329 (3)	0.061
C33	−0.4675 (5)	−0.3695 (4)	−0.1215 (3)	0.045
C34	−0.6065 (6)	−0.4342 (5)	−0.1476 (3)	0.058
C35	−0.6452 (6)	−0.5070 (5)	−0.2049 (4)	0.064
C36	−0.5462 (8)	−0.5156 (5)	−0.2362 (3)	0.061
C37	−0.4105 (7)	−0.4523 (5)	−0.2122 (3)	0.063
C38	−0.3680 (6)	−0.3794 (4)	−0.1537 (3)	0.054
C39	−0.5391 (5)	−0.2949 (4)	−0.0001 (3)	0.045
C40	−0.5049 (6)	−0.3157 (5)	0.0682 (3)	0.067
C41	−0.6043 (8)	−0.3390 (6)	0.1077 (3)	0.096
C42	−0.7357 (7)	−0.3463 (5)	0.0775 (4)	0.088
C43	−0.7707 (6)	−0.3242 (5)	0.0101 (3)	0.067
C44	−0.6714 (6)	−0.2968 (4)	−0.0285 (3)	0.055
C45	−0.3944 (5)	−0.1453 (4)	−0.0878 (3)	0.047
C46	−0.3740 (7)	−0.1324 (5)	−0.1534 (3)	0.071
C47	−0.3607 (8)	−0.0372 (6)	−0.1808 (4)	0.090
C48	−0.3661 (7)	0.0428 (5)	−0.1423 (5)	0.077
C49	−0.3844 (7)	0.0323 (5)	−0.0769 (4)	0.091
C50	−0.3975 (7)	−0.0627 (5)	−0.0482 (3)	0.077

[a] Equivalent isotropic temperature factor U_{eq} (Å^2) defined as one-third of the trace of the orthogonalized U_{ij} tensor.

into the Mo=S unit could initially give a trithiocarbonate ligand that, following intramolecular S addition, is converted to the perthiocarbonate ligand; alternatively, S_2 dissociation from the Mo-η^2-S_4 unit affords the Mo-η^2-S_2 unit that directly inserts CS_2 to form the perthiocarbonate ligand. The dissociation of S_2 from Mo-coordinated S_4 ligands is well established and in the $[(L)_2Mo(E)(\mu\text{-}S)_2Mo(E)(S_4)]^{2-}$ complexes (E = S, O) is influenced by distant electronic effects, due to the equatorial terminal

Table VI. Fractional Atomic Coordinates and Thermal Parameters for $[Et_4N]_2[Mo_2(O)_2(\mu\text{-}S)_2(\eta^2\text{-}CS_4)(\eta^2\text{-}CS_3)]$ (V)

atom	x	y	z	U^a
Mo1	0.3675 (1)	0.6516 (0)	0.8287 (1)	0.044
Mo2	0.2278 (1)	0.6505 (0)	0.6887 (1)	0.047
S1	0.1903 (4)	0.6421 (1)	0.8321 (3)	0.051
S2	0.4003 (4)	0.6326 (1)	0.6858 (3)	0.049
S3	0.5230 (4)	0.6113 (2)	0.8403 (4)	0.062
S4	0.3375 (4)	0.6250 (2)	0.9725 (4)	0.062
S5	0.5580 (5)	0.6010 (2)	0.9679 (5)	0.086
S6	0.4457 (6)	0.5938 (2)	1.1247 (6)	0.120
S7	0.2209 (5)	0.6126 (2)	0.5524 (4)	0.073
S8	0.0619 (5)	0.6158 (2)	0.6728 (4)	0.073
S9	0.0156 (6)	0.5773 (2)	0.5031 (5)	0.103
O1	0.3960 (10)	0.7027 (3)	0.8409 (8)	0.061
O2	0.2121 (10)	0.7010 (4)	0.6627 (8)	0.065
C1	0.4539 (14)	0.6054 (5)	1.0215 (10)	0.044
C2	0.0913 (17)	0.6017 (7)	0.5700 (15)	0.080
N1	0.4553 (11)	0.2558 (4)	0.4243 (9)	0.039
C3	0.4488 (17)	0.2174 (5)	0.4781 (14)	0.067
C4	0.3623 (20)	0.2164 (6)	0.5427 (15)	0.082
C5	0.4748 (17)	0.2948 (5)	0.4791 (14)	0.069
C6	0.5707 (20)	0.2948 (6)	0.5329 (14)	0.078
C7	0.3577 (16)	0.2594 (6)	0.3724 (15)	0.074
C8	0.3555 (18)	0.2967 (7)	0.3101 (15)	0.096
C9	0.5457 (17)	0.2509 (6)	0.3632 (14)	0.070
C10	0.5409 (18)	0.2154 (6)	0.2978 (14)	0.079
N2	0.2500 (0)	0.0 (0)	0.3023 (12)	0.044
C11	0.1901 (17)	0.0317 (7)	0.2501 (14)	0.076
C12	0.1109 (19)	0.0111 (7)	0.1892 (15)	0.091
C13	0.3298 (17)	0.0251 (6)	0.3568 (14)	0.072
C14	0.3955 (19)	−0.0036 (8)	0.4121 (15)	0.089
N3	0.2500 (0)	0.5000 (0)	0.3045 (16)	0.070
C15	0.3277 (38)	0.4953 (15)	0.2249 (31)	0.095
C16	0.2500 (0)	0.5000 (0)	0.1443 (33)	0.161
C17	0.3304 (38)	0.4980 (15)	0.3799 (31)	0.090
C18	0.2500 (0)	0.5000 (0)	0.4641 (26)	0.120
C19	0.1718 (36)	0.4624 (14)	0.3152 (29)	0.077
C20	0.2402 (20)	0.4181 (8)	0.3091 (15)	0.100
C21	0.3216 (31)	0.4622 (12)	0.3057 (25)	0.058

[a] Equivalent isotropic temperature factor U_{eq} (Å^2) defined as one-third of the trace of the orthogonalized U_{ij} tensor.

ligands (L) on the second Mo atom.[2] At present, it is difficult to ascertain which of the two pathways (Figure 5) is more likely, and either of the two (or both) may be operative. Under mild conditions, i.e. gentle heating or applying vacuum at ambient temperature, the $[Mo_2(S)_2(\mu\text{-}S)_2(\eta^2\text{-}CS_4)_2]^{2-}$ complex, III, loses CS_2 to give the known[17] $[Mo_2(S)_2(\mu\text{-}S)_2(\eta^2\text{-}S_2)_2]^{2-}$ complex. Regeneration of III is achieved by CS_2 addition to the latter complex. The CS_4^{2-} ligands in I and II also readily lose CS_2. Upon standing at ambient temperature for 7 h, CH_3CN or DMF solutions of either I or II reach limiting electronic spectra. Identical spectra are obtained when these solutions are placed under vacuum for 1 h. Addition of CS_2 to these solutions regenerates the characteristic electronic spectra of a mixture of I and II. A solid product can be isolated from the partially CS_2-depleted solutions and shows a strong C=S vibration in the infrared spectrum. This product is postulated to be mainly the $[Mo(S)(S_2)(CS_4)]^{2-}$ complex. Upon extended standing (>12 h), DMF solutions of I and II give only III. The formation of III may be due to a solvent-assisted self-coupling reaction of the postulated $[Mo(S)(S_2)(CS_4)]^{2-}$ complex followed by reductive S–S bond cleavage (Figure 6). Attempts to obtain the $[(S)Mo(\eta^2\text{-}CS_3)_2]^{2-}$ complex in reactions of either I or II with Ph_3P yielded Ph_3PS, but a pure, single Mo/S complex could not be obtained in these reactions. The syntheses of IV from either the reaction of CS_2 with $[Mo_2S_6]^{2-}$ or the reaction of Ph_3P with III are based on well-known[11] reactions.

The reluctance of the remaining free Mo=S groups in I, II, III, or IV to react further with CS_2 may signify a sufficient

(17) (a) Miller, K. F.; Bruce, A. E.; Corbin, J. L.; Wherland, S.; Stiefel, E. I. *J. Am. Chem. Soc.* **1980**, *102*, 5102. (b) Pan, W. H.; Harmer, M. A.; Halbert, T. R.; Stiefel, E. I. *J. Am. Chem. Soc.* **1984**, *106*, 459.

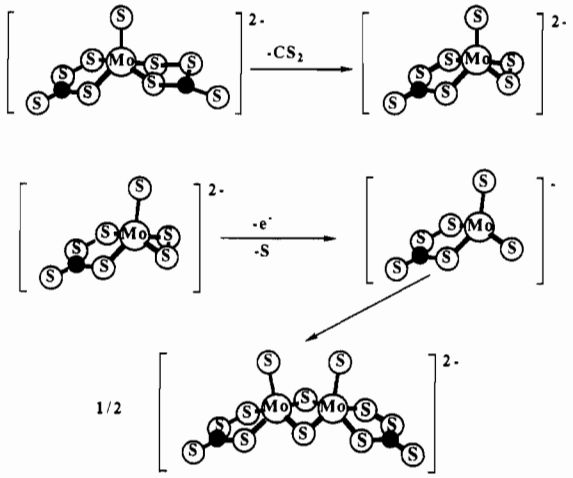

Figure 6. Possible mechanism for the formation of the $[Mo_2(S)_2(\mu\text{-}S)_2(\eta^2\text{-}CS_4)_2]^{2-}$ dimer from the $[(S)Mo(\eta^2\text{-}CS_4)_2]^{2-}$ complexes.

inactivation of these groups to further react with CS_2, a rather weak electrophile. This behavior contrasts with the addition reactions observed with the strongly electrophilic, activated alkynes where all of the Mo=S groups react. Thus, in the anaerobic reaction of $[(S)Mo(\eta^2\text{-}S_4)_2]^{2-}$ with DMA, the final product is the $[Mo^{IV}(DMDA)_3]^{2-}$ dithiolene. The analogous $[Mo^{IV}(CS_4)_2(CS_3)]^{2-}$ complex, that may have been obtained if I or II had reacted further with CS_2, does not form.

The synthesis of V from the reaction of $[(S)Mo(O)(\mu\text{-}S)Mo(O)(S_4)]^{2-}$ with CS_2 can be visualized as an outcome of reactions consistent with the known solution behavior of the Mo-η^2-S_4 and Mo-η^2-S_2 functional groups:[6]

$$[(S)Mo(O)(\mu\text{-}S)_2Mo(O)(S_4)]^{2-} + CS_2 \rightarrow [(CS_3)Mo(O)(\mu\text{-}S)_2Mo(O)(S_4)]^{2-} \quad (1)$$

$$[(CS_3)Mo(O)(\mu\text{-}S)_2Mo(O)(S_4)]^{2-} \rightarrow [(CS_3)Mo(O)(\mu\text{-}S)_2Mo(O)(S_2)]^{2-} + \tfrac{2}{8}S_8 \quad (2)$$

$$[(CS_3)Mo(O)(\mu\text{-}S)_2Mo(O)(S_2)]^{2-} + CS_2 \rightarrow [(CS_3)Mo(O)(\mu\text{-}S)_2Mo(O)(CS_4)]^{2-} \quad (3)$$

The synthesis of V from $[(S_2)Mo(O)(\mu\text{-}S)_2Mo(O)(S_4)]^{2-}$ is not as straightforward and necessitates either the presence of an intermediate with a Mo=S group or the ready loss of sulfur from one of the perthiocarbonate ligands in the anticipated $[(CS_4)Mo(O)(\mu\text{-}S)_2Mo(O)(CS_4)]^{2-}$ complex. The preferential reactivity of the (O)Mo=S group toward CS_2, relative to the (O)Mo(S_4) group (eq 1), is demonstrated by the controlled reaction of CS_2 with $[(S)Mo(O)(\mu\text{-}S)_2Mo(O)(S_4)]^{2-}$. The latter, obtained in situ by sulfur abstraction from $[(S_2)Mo(O)(\mu\text{-}S)_2Mo(O)(S_4)]^{2-}$ with Ph_3P, when treated with CS_2 for a short period of time affords only $[(CS_3)Mo(O)(\mu\text{-}S)_2Mo(O)(S_4)]^{2-}$. This complex can be isolated as the Et_4N^+ salt, VI, in excellent yield as described previously,[2] and its analytical and spectroscopic characteristics are consistent with the proposed formulation (see Experimental Section and Table VIII).

Structures. The structures of the *trans*- and *cis*-$[(S)Mo^{IV}(\eta^2\text{-}CS_4)_2]^{2-}$ anions in I and II, respectively, are shown in Figures 1 and 2. In both complexes, the Mo(IV) atom is bound to a terminal sulfide ligand (2.163 (3) Å). The S donors of the bidentate CS_4^{2-} ligands define the base of the slightly distorted rectangular, (S)MoS_4, pyramid. The distortions that give rise to a slightly trapezoidal base in II and a parallelepipedal base in I are due to the unequal Mo–S bond lengths in the equatorial plane (vide infra). The Mo=S thiomolybdenyl unit lies on the axis normal to the base, and the Mo atom is displaced from the rectangular S_4 plane toward the sulfido group by 0.749 (1) Å in I and by 0.720 (1) Å in II. The Mo–S distances in both I and II are divided metrically into two sets. The Mo–S distances in I are 2.320 (3), 2.333 (3), 2.386 (3), and 2.380 (3) Å whereas in II

Table VII. Summary of Interatomic Distances and Angles for *trans*-$[Ph_4P]_2[Mo(S)(CS_4)_2]$·DMF (I), *cis*-$[Ph_4P][Et_4N][Mo(S)(CS_4)_2]$ (II), *cis-syn*-$[Ph_4P]_2[Mo_2(S)_2(\mu\text{-}S)_2(CS_4)_2]\cdot{}^1/_2$DMF (III), *syn*-$[Ph_4P]_2[Mo_2(S)_2(\mu\text{-}S)_2(CS_3)_2]$ (IV), and *syn*-$[Et_4N]_2[Mo_2(O)_2(\mu\text{-}S)_2(CS_4)(CS_3)]$ (V)[a]

	I	II	III	IV	V
			Distances,[b] Å		
Mo–Mo			2.840 (3)	2.823 (1)	2.835 (2)
Mo–S_b			2.316 (5)	2.300 (7)	2.305
range			2.310 (6)–2.326 (5)	2.287 (1)–2.316 (2)	2.297 (5), 2.314 (5)
Mo–S_b[c]					2.333
range					2.325 (5), 2.341 (5)
Mo=S	2.126 (3)	2.127 (4)	2.108	2.100	
range			2.108 (5), 2.108 (5)	2.092 (2), 2.108 (2)	
Mo=O					1.678
range					1.672 (13), 1.684 (9)
Mo–S_L	2.383	2.376 (3)	2.413	2.433 (8)	2.433 (6)
range	2.380 (3), 2.386 (3)		2.408 (5)–2.418 (6)	2.416 (1)–2.447 (2)	2.421 (6)–2.440 (5)
Mo–S–S_L	2.326	2.320 (3)	2.391		2.401 (5)
range	2.320 (3), 2.333 (3)		2.390 (6)–2.393 (6)		
C–S_L	1.74	1.756 (10)	1.78	1.731 (7)	1.75 (3)
range	1.735 (12), 1.739 (12)		1.74 (2), 1.82 (2)	1.725 (5)–1.739 (7)	1.70 (2)–1.81 (2)
C–S–S_L	1.71	1.726 (11)	1.69		1.60 (2)
range	1.719 (12), 1.709 (12)		1.69 (2), 1.69 (2)		
C=S[d]	1.65	1.615 (9)	1.61		1.65 (2)
range	1.640 (11), 1.662 (11)		1.54 (2), 1.68 (2)		
C=S[e]				1.625	1.63 (2)
range				1.622 (6), 1.627 (6)	
S–S	2.101 (5)	2.105 (4)	2.005		2.061 (9)
range	2.102 (5), 2.100 (5)		1.995 (10), 2.016 (9)		
			Angles, deg		
Mo–S_b–Mo			75.6	75.6	75.4
range			75.5 (1), 75.8 (1)	75.3 (1), 76.0 (1)	75.0 (2), 75.7 (2)
S_b–Mo–S_b			101.4	100.8	100.5
range			101.3 (3), 101.6 (3)	100.8 (1), 100.9 (1)	99.7 (2), 101.3 (2)
S_L–Mo–S_L[f]	86.4 (1)	85.72 (12)	82.9	70.0	76.5
range	86.70 (14), 86.00 (13)		85.5 (2), 83.4 (2)	69.9 (1), 70.0 (1)	69.8 (2), 83.1 (2)
S–S_L–Mo–$S_t(O_t)$	109.8 (2)	110.2 (2)	108.4		108.9 (5)
range	109.4 (2), 110.1 (2)		107.4 (3), 109.5 (3)		
S_L–Mo–$S_t(O_t)$	107.4 (2)	107.8 (2)	105.5	107.3 (1)	106.2 (5)
range	107.6 (2), 107.2 (2)		105.4 (3), 105.7 (3)	104.7 (1)–109.8 (1)	105.2 (5)–107.7 (5)
S_b–Mo–$S_t(O_t)$			108.5 (5)	109.6 (1)	109.4 (5)
range			107.2 (3), 108.8 (3)	108.1 (1)–112.2 (1)	108.4 (5)–110.5 (5)

[a] Mean values of crystallographically independent, chemically equivalent structural parameters. The number in parentheses represents the larger of the individual standard deviations for the standard deviation from the mean, σ:

$$\sigma = \sqrt{\sum_{i=1}^{N}(x_i - \bar{x})^2/N(N-1)}$$

[b] Structural information on the counterions is as follows. III: cation P1, P–C range 1.78 (2)–1.79 (2), mean P–C 1.79 (2), C–C range 1.29 (2)–1.41 (3), mean C–C 1.38 (3); cation P2, P–C range 1.77 (2)–1.80 (2), mean P–C 1.78 (2), C–C range 1.26 (3)–1.45 (4), mean C–C 1.37 (4). IV: cation P1, P–C range 1.78 (1)–1.80 (1), mean P–C 1.79 (1), C–C range 1.36 (1)–1.40 (1), mean C–C 1.38 (2). V: cation N1, N–C range 1.49 (2)–1.53 (2), mean N–C 1.51 (2), C–C range 1.50 (3)–1.53 (3), mean C–C 1.52 (3); cation N2, N–C range 1.51 (2)–1.56 (2), mean N–C 1.54 (2), C–C range 1.52 (3)–1.55 (3), mean C–C 1.53 (3); cation N3, N–C range 1.52 (4)–1.60 (5), mean N–C 1.57 (5), C–C range 1.62 (6)–1.76 (4), mean C–C 1.67 (6). [c] Mo bound to the CS_4^{2-} ligand. [d] C=S bond in the CS_4^{2-} ligand. [e] C=S bond in the CS_3^{2-} ligand. [f] Intraligand.

Table VIII. Infrared, ^{13}C NMR, and Electronic Spectral Data for *trans*-$[Ph_4P]_2[(S)Mo(\eta^2\text{-}CS_4)_2]$ (I), *cis*-$[Ph_4P][Et_4N][(S)Mo(\eta^2\text{-}CS_4)_2]$ (II), *syn-cis*-$[Ph_4P]_2[Mo_2(S)_2(\mu\text{-}S)_2(\eta^2\text{-}CS_4)_2]\cdot{}^1/_2$DMF (III), *syn*-$[Ph_4P]_2[Mo_2(S)_2(\mu\text{-}S)_2(\eta^2\text{-}CS_3)_2]$ (IV), *syn*-$[Et_4N]_2[Mo_2(O)_2(\mu\text{-}S)_2(\eta^2\text{-}CS_4)(\eta^2\text{-}CS_3)]$ (V), *syn*-$[Et_4N]_2[Mo_2(O)_2(\mu\text{-}S)_2(\eta^2\text{-}S_4)(\eta^2\text{-}CS_3)]$ (VI), *syn*-$[Et_4N]_2[Mo_2(O)_2(\mu\text{-}S)_2(\eta^2\text{-}S_2)(\eta^2\text{-}CS_3)]$ (VII), and *syn*-$[Et_4N]_2[Mo_2(O)_2(\mu\text{-}S)_2(\eta^2\text{-}CS_3)_2]$ (VIII)

compd	ν(Mo–O(S))[a]	ν(Mo–S_b)	ν(C=S)	^{13}C NMR,[b] δ	electronic data,[c] nm
I			980 (s)	245.6, 246.0	430, 334
II			977 (s)	245.6, 246.0	430 (sh), 393, 335
III		464 (w)	982 (ms)	235.2, 237.2	610 (sh), 470 (sh), 365 (sh), 314 (sh)
IV		460 (w)	1052 (s)	252.8[d]	444 (sh), 344
V	950 (s)	469 (m)	982 (m), 1054 (m)	244.5, 251.3[d]	460, 374 (sh)
VI	949 (vs)	468 (m)	1058 (vs)	252[d]	310 (sh), 258 (sh)
VII	952 (vs)	479 (w)	1051 (s)	255	460, 380 (sh), 330 (sh)
VIII	947 (s), 934 (mw)	470 (w)	1046 (vs)	253	450

[a] Obtained in KBr disks. [b] Obtained in CD_3CN solution. [c] Obtained in DMF solution. [d] Obtained in DMSO-d_6 solution.

the analogous distances are 2.320 (3) and 2.376 (3) Å. The shorter Mo–S distances always are found with the sulfur atoms of the disulfide unit of the CS_4^{2-} ligand. This places the shorter Mo–S distances cis to each other in the cis anion in II and trans to each other in the trans anion in I. *The structural characteristics of I and II definitely rule out a trans effect as the origin of the unequal Mo–S bond lengths in either I or II. Instead, the long S–S bonds in the coordinated CS_4^{2-} ligands in I and II, at 2.105 (5) and 2.105 (4) Å, respectively, support the contention that significant p_π–d_π bonding in the shorter Mo–S bonds is augmented at the expense of the p_π–p_π bonding in the S–S bonds adjacent to them.* A similar asymmetry in the Mo–S bond lengths (that may be attributed to similar π-bonding effects) has been found previously in the structure of the $[(S)Mo^{IV}(\eta^2\text{-}S_4)_2]^{2-}$ anion,[10]

which shows both short and long equatorial Mo–S distances of 2.331 (1) and 2.387 (1) Å. The average intraligand S–S distances of 3.223 (8) and 3.195 (4) Å in I and II, respectively, are shorter than those found in the structure of the $[(S)Mo^{IV}(\eta^2\text{-}S_4)_2]^{2-}$ anion (3.345 (1) Å). As a consequence, the interligand S–S distances in I and II at 3.09 and 3.08 Å are longer than that in the $[(S)Mo^{IV}(\eta^2\text{-}S_4)_2]^{2-}$ anion (2.984 (1) Å). These findings reinforce the argument that interligand S–S distances may be dictated primarily by the ligand bite size rather than by interligand S–S (bonding) contacts. The dimensions of the CS_4^{2-} ligands in I and II (Table VII) generally are similar to those found in the "localized" CS_4^{2-} anion in $K_2CS_4{\cdot}CH_3OH$[18] but are characterized by unusually long S–S bonds. The lengthening of these bonds, by comparison to those in $Ni(CS_4)_2^{2-}$ (2.063 (3) Å)[19] or the free CS_4^{2-} ligand[18] (2.021 Å), as argued previously,[1] may be rationalized in terms of a weakening of the π bonding. The influence of Mo–S π bonding in weakening the S–S bond, apparent in the S_4^{2-} and CS_4^{2-} ligands, also is found in the perthioarylato ligands in the structures of the $[Mo^{IV}(O)(S_2CPh)(S_3CPh)]$[20] and the $[Fe^{III}(S_2C\text{-}p\text{-}Me\text{-}Ph)_2(S_3C\text{-}p\text{-}MePh)]$ complexes.[21] The Mo dithiobenzoate–perthiobenzoate complex contains two Mo–S bonds at 2.416 (1) and 2.376 (1) Å, and the shorter bond is located adjacent to the S–S bond. The S–S distance of the perthiobenzoate ligand, at 2.048 (1) Å, is appreciably longer than the S–S bonds in the bis(perthiobenzoato)zinc(II)[22] and the bis(perthiocumato)zinc(II)[23] complexes, at 2.007 and 2.008 Å, respectively. Similarly, the Fe complex shows[21] two Fe–S bonds associated with the perthio ligand, at 2.184 (7) and 2.238 (7) Å, and a rather long S–S bond, at 2.086 (8) Å.

The $[Ph_4P]_2[syn\text{-}cis\text{-}Mo_2(S)_2(\mu\text{-}S)_2(\eta^2\text{-}CS_4)_2]{\cdot}{}^1/_2DMF$ complex (III) is X-ray isomorphous with the $[Ph_4P]_2[Mo_2S_{10.56}]$ complex and contains a similar $[Mo_2S_4]^{2+}$ core with two $[Mo^V{=}S]^{3+}$ units bridged by two S^{2-} ligands. The coordination sphere of each of the rectangular pyramidal molybdenum atoms is completed by a bidentate CS_4^{2-} ligand, and the two CS_4^{2-} ligands in III are disposed in a cis configuration relative to each other. The two distorted MoS_5 units in III are linked by edge sharing in the syn configuration, and the Mo atoms are located above the basal sulfur planes by 0.721 (2) and 0.717 (2) Å. The Mo–S_b distances in III (Mo_1–S_b = 2.31, Mo_2–S_b = 2.32 Å) do not show the asymmetry found in the bridging unit of the $[Mo_2S_{10.56}]^{2-}$ anion. The CS_4^{2-} ligands in III show a localization of charge not unlike that found in other CS_4^{2-} complexes (Table VII), including the $[Ni(CS_4)_2]^{2-}$ complex.[19] The asymmetry in the Mo–S_L bonds and the lengthening of the ligand S–S bonds found in the structures of I and II are not apparent in III, where the higher formal oxidation state of the Mo atoms (and weaker reducing character) apparently results in less pronounced Mo–S d_π–p_π bonding. The structures of the anions in $[Ph_4P]_2[syn\text{-}Mo_2(S)_2(\mu\text{-}S)_2(\eta^2\text{-}CS_3)_2]$ (IV) and $[Et_4N]_2[Mo_2(O)_2(\mu\text{-}S)_2(\eta^2\text{-}CS_4)(\eta^2\text{-}CS_3)]$ (V) are very similar to the structures of the anion in III. In IV, the two distorted square pyramidal MoS_5 units are linked by edge sharing in the syn configuration, with the Mo atoms elevated above the equatorial sulfur planes by 0.749 and 0.756 Å. The two $MoS_2C{=}S$ units are nearly planar, with deviations from planarity of less than 0.1 and 0.02 Å. In V, the MoS_5 structural subunits are disposed similarly to those in IV and show the Mo atoms elevated from the basal planes by 0.741 and 0.747 Å. The $MoS_2C{=}S$ and $MoS_3C{=}S$ subunits also are very nearly planar, with deviations from planarity of less than 0.1 Å. The Mo=O bond lengths of 1.67 (1) and 1.68 (1) Å are quite normal by comparison to other previously characterized oxo–Mo(V) complexes.[24]

The only significant differences between IV and V and III arise as a consequence of the structural differences between the CS_3^{2-} ligands in IV and V and the CS_4^{2-} ligands in III. In IV and V, the smaller intraligand S–S distances, "bites", in the CS_3^{2-} ligands result in acute S_L–Mo–S_L angles of 70.0 (1) and 69.8 (2)°, respectively, when compared to the corresponding angles in III, at 82.9°. All other bond lengths and angles in IV and V (Table VII) are very similar to corresponding structural features in III.

Spectroscopic Properties. The vibrational infrared, ^{13}C NMR, and electronic spectra of the complexed are compiled in Table VIII. In the infrared spectra of the dimeric Mo(V) complexes, the Mo–S_b vibration occurs as a weak band around 470 cm^{-1}. The energy of the C=S vibration of the coordinated CS_3^{2-} ligands invariably is lower (~980 cm^{-1}) than that of the C=S vibration in the CS_4^{2-} complexes (~1050 cm^{-1}). On the basis of the C=S vibrational frequencies, the presence of either of the two ligands can be ascertained with considerable confidence. An additional diagnostic indicator for the CS_3^{2-} and CS_4^{2-} ligands is the characteristic ^{13}C NMR resonance associated with each of the two ligands. Generally, this resonance is found near 246 ppm for the Mo-coordinated CS_4^{2-} ligands and around 253 ppm for the Mo-coordinated CS_3^{2-} ligands. Two ^{13}C resonances are observed for I–III in solution. The chemical shifts indicate that they originate from perthiocarbonate ligands. For I and II, these resonances very likely indicate the presence of both cis and trans isomers in solution. For III, cis and trans isomers also are possible in solution; however, the additional possibility of syn and anti isomers further complicates the issue and precludes a reliable assignment.

Solution Behavior. The complex equilibria that prevail in DMSO solutions that contain Mo/S(O)–perthiocarbonate complexes were revealed by ^{13}C NMR spectroscopy. The ^{13}C NMR spectrum of VI was obtained periodically over a 2-week interval, and the results are shown in Figure 7. The resonances that are due to the Mo-coordinated CS_3^{2-} or CS_4^{2-} ligands increase in number with time, yellow crystals of elemental sulfur deposit on the walls of the sample container, and the ^{13}C resonance of free CS_2 eventually makes its appearance. A sequence of events that accounts for these changes can be advanced (Figure 8), and most of the ^{13}C NMR resonance assignments are based on data obtained from separately obtained "authentic" complexes.

The initial tetrasulfido species $[Mo_2O_2S_2(CS_3)(S_4)]^{2-}$, VI (252 ppm, Figure 8; spectrum 1, Figure 7) transforms to the disulfido species $[Mo_2O_2S_2(CS_3)(S_2)]^{2-}$, VII (255 ppm, Figure 8; spectrum 1, Figure 7) by dissociating elemental sulfur. Indeed, the single yellow crystals that appear at this time have been identified positively as elemental sulfur. The assignment of the 255 ppm resonance to VII (Figures 7 and 8) is supported by the presence of an identical resonance in the ^{13}C NMR spectrum of pure VII synthesized separately by the reaction of $[Mo_2O_2S_2(DMF)_3]$ with Na_2CS_3 (see Experimental Section). Evidence for sulfur dissociation and transformation of the tetrasulfido ligand to the disulfido ligand has been obtained previously in a ^1H NMR study of the $[Mo_2O_2S_2(Cp)(S_4)]^{2-}/[Mo_2O_2S_2(Cp)(S_2)]^{2-}$ equilibrium system.[3,6] After 27 h, a new resonance appears at 253 ppm. This resonance (Figure 7, spectrum 2) can be attributed to the $[Mo_2O_2S_2(CS_3)(CS_3)]^{2-}$ complex, VIII, and is identical to that obtained for an "authentic" sample of VIII. The latter was obtained rationally by the reaction of the $[Mo_2O_2S_2(DMF)_6][I]_2$[12] complex with Na_2CS_3. At this time, we can only speculate that the formation of VIII is due to a ligand-exchange reaction between VI and VII to form VIII and the ^{13}C NMR "silent" $[Mo_2O_2S_2(S_2)(S_4)]^{2-}$ complex. The reaction between VI and VII apparently is faster than the insertion of elemental sulfur into the CS_3^{2-} ligand of VII and the formation of the perthiocarbonate derivative IX (246 ppm, Figure 8; spectrum 3, Figure 7). The formation of IX becomes evident by a resonance at 246 ppm that appears in about a week and after the 253 ppm resonance, characteristic of VIII, has appeared in the spectrum. Addition of elemental sulfur to, and transformation of, the trithiocarbonate ligand CS_3^{2-} to the

(18) Bueno, W. A.; Lautie, A.; Sourisseau, C.; Zins, D.; Robineau, M. *J. Chem. Soc., Perkin Trans.* **1978**, 1011.
(19) Coucouvanis, D.; Patil, P. R.; Kanatzidis, M. G.; Detering, B.; Baenziger, N. C. *Inorg. Chem.* **1985**, *24*, 24.
(20) Tatsumisago, M.; Matsubayashi, G.; Tanaka, T. *J. Chem. Soc., Dalton Trans.* **1982**, 121.
(21) Coucouvanis, D.; Lippard, S. J. *J. Am. Chem. Soc.* **1969**, *91*, 307.
(22) Bonamico, M.; Dessy, G.; Fares, V.; Scaramuzza, L. *J. Chem. Soc. A* **1971**, 3191.
(23) Fackler, J. P., Jr.; Fetchin, J. A.; Fries, D. C. *J. Am. Chem. Soc.* **1972**, *94*, 7323.
(24) Bunzey, G.; Enemark, J. H. *Inorg. Chem.* **1978**, *17*, 682.

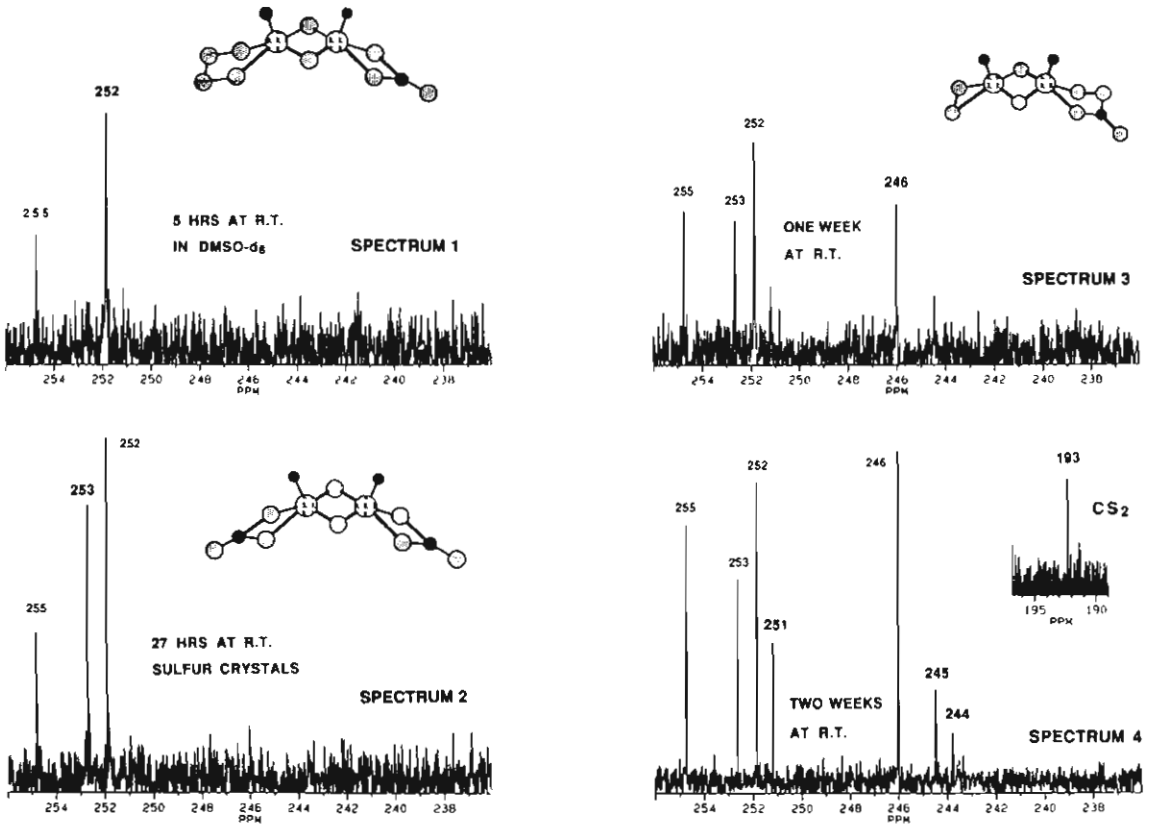

Figure 7. ^{13}C NMR spectra of the $[Mo_2(O)_2(\mu\text{-}S)_2(\eta^2\text{-}CS_4)(\eta^2\text{-}S_4)]^{2-}$ anion in dimethyl sulfoxide solution at ambient temperature monitored over 2 weeks.

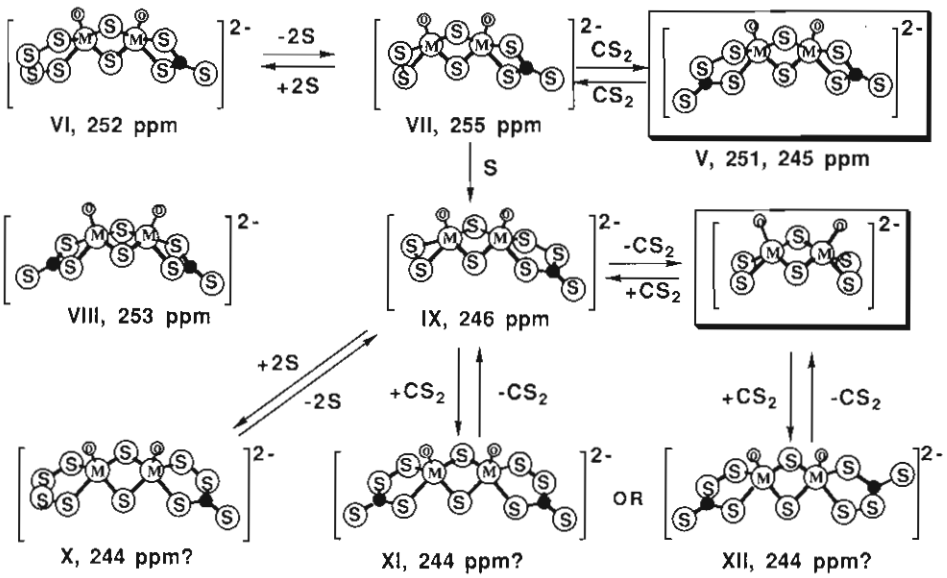

Figure 8. Solution behavior of the Mo–perthiocarbonate complexes as suggested by ^{13}C NMR spectroscopy.

perthiocarbonate CS_4^{2-} ligand has been demonstrated previously.[16]

As indicated above, the assignment of the ^{13}C NMR resonances is assisted by the general observation that the perthiocarbonate ligands show resonances higher upfield from those found with the trithiocarbonate ligands. Specifically, the resonances of the perthiocarbonate ligands for V and IX at 245 and 246 ppm, respectively, are distinct from those of the trithiocarbonate ligands for VI–VIII at 252, 255, and 253 ppm, respectively. This observation also is consistent with the ^{13}C NMR spectra of the $[Mo_2O_2S_2(L)(Cp)]^-$ complexes.[2] For the latter, ^{13}C resonances are found at 247 and 255 ppm for $L = CS_4^{2-}$ and CS_3^{2-}, respectively.

The loss of CS_2 from the coordinated CS_4^{2-} ligand in IX to form $[Mo_2O_2S_2(S_2)_2]^{2-}$ is suggested by the presence of free CS_2 with a resonance at 193 ppm (Figure 7, spectrum 4). The free CS_2 in solution can add to VII with formation of the $[Mo_2O_2S_2(CS_4)(CS_3)]^{2-}$ complex, V. The presence of the latter is identified by two resonances that appear at 245 and 251 ppm, after ca. 2 weeks. This assignment is supported by the observation that the same two resonances are found in the spectrum of "authentic" V. Addition of CS_2 to IX or $[Mo_2O_2S_2(S_2)_2]^{2-}$ can give perthiocarbonate complexes such as XI or XII (Figure 7). The latter may account for the unassigned resonance at 244 ppm (Figures 7 and 8). The 244 ppm resonance also could arise from a perthiocarbonate complex such as X, which forms by the addition of sulfur to the η^2-S_2 ligand in IX.

Conclusions

The formation of Mo-coordinated perthiocarbonate ligands occurs as a result of CS_2 insertion into Mo-η^2-S_2 units or by intra-

or intermolecular sulfur addition to Mo-coordinated CS_3^{2-} ligands. The latter are obtained by CS_2 addition to the Mo=S functional groups and are quite stable in the absence of available sulfur. In contrast to the Mo-η^2-CS_3 units that do not readily dissociate CS_2, the Mo-η^2-CS_4 chromophores are quite unstable in solution and readily dissociate CS_2 with formation of the Mo-η^2-S_2 units. Unlike the pronounced reactivity of "activated" alkynes such as dicarbomethoxyacetylene (DMA), which add to all available Mo=S bonds within a thiomolybdate complex, CS_2 reacts only partially. This is illustrated in the reactions of $[Mo_2S_{10/12}]^{2-}$ with these electrophilic molecules. The reaction of DMA with all, nonbridging, Mo-S_x groups in $[Mo_2S_{10/12}]^{2-}$ results in the formation of the previously reported[2] $[Mo_2S_2(S_2C_2(CO_2Me)_2)_4]^{2-}$ dithiolene complex. In contrast, the reaction with CS_2 affords III, which contains two "unreacted" Mo=S groups. At this time, we can only speculate that introduction of CS_3^{2-} or CS_4^{2-} ligands into the thiomolybdate complexes (by CS_2 addition to the Mo-S_x sites) reduces the nucleophilicity of the remaining Mo=S groups, which appear incapable of reacting further with the weakly electrophilic CS_2 molecule. The observed lack of reactivity of CS_2 with the Mo=O groups in the thiomolybdate complexes is consistent with previous studies[2,3a] of the reactions of DMA with thiomolybdate complexes and underscores the complete lack of reactivity of the Mo=O group in these complexes, at least toward electrophilic carbon sites.

At present, we are exploring the reactivity of the Mo=S and Mo—η^2-S_2 groups with other electrophiles, and in the near future, we will report[5] on the chemistry of the thiomolybdate complexes with SO_2.

Acknowledgment. The support of this work by a grant from the National Science Foundation (CHE-9006069) is gratefully acknowledged.

Supplementary Material Available: Tables S1-S5, containing listings of positional parameters, thermal parameters, and selected distances and angles of $[Ph_4P]_2[trans\text{-}(S)Mo(\eta^2\text{-}CS_4)_2]\cdot DMF$ (I), $[Ph_4P][Et_4N][cis\text{-}(S)Mo(\eta^2\text{-}CS_4)_2]$ (II), $[Ph_4P]_2[syn\text{-}cis\text{-}Mo_2(S)_2(\mu\text{-}S)_2(\eta^2\text{-}CS_4)_2]\cdot{}^1/_2DMF$ (III), $[Ph_4P]_2[syn\text{-}Mo_2(S)_2(\mu\text{-}S)_2(\eta^2\text{-}CS_3)_2]$ (IV), and $[Et_4N]_2[Mo_2(O)_2(\mu\text{-}S)_2(\eta^2\text{-}CS_4)(\eta^2\text{-}CS_3)]$ (V) (41 pages); Tables S6-S9, listing calculated and observed structure factors for I, IV, V, and II (116 pages). Ordering information is given on any current masthead page. Crystallographic data for the $[Ph_4P]_2[syn\text{-}cis\text{-}Mo_2(S)_2(\mu\text{-}S)_2(\eta^2\text{-}CS_4)_2]\cdot{}^1/_2DMF$ complex already have been deposited with a previous communication.[4]

Contribution from the Institut für Physikalische und Theoretische Chemie and Physikalisches Institut, University of Erlangen-Nürnberg, D-8520 Erlangen, Germany, and Department of Chemistry, University of Surrey, Guildford GU2 5XH, Great Britain

Rapid versus Intermediate Electronic Relaxation between $S = {}^3/_2$ and $S = {}^1/_2$ States in Nitrosyl-Iron Complexes with Jäger-Type Ligands

E. König,*[,1] G. Ritter,[2] J. Dengler,[2] and L. F. Larkworthy[3]

Received April 15, 1991

The spin-state transitions between low-spin ($S = {}^1/_2$) and intermediate-spin ($S = {}^3/_2$) states in the complexes [Fe(J·ph)NO] and [Fe(J·mph)NO] with Jäger-type ligands have been studied between 80 and 320 K on the basis of magnetism, ^{57}Fe Mössbauer effect, and X-ray powder diffraction. The transition in [Fe(J·ph)NO] is centered at $T_c \simeq 143$ K, the electronic relaxation between the spin states being rapid with $\tau \lesssim 1 \times 10^{-8}$ s at all temperatures. The transition in [Fe(J·mph)NO] is centered at $T_c \simeq 187$ K, the line shapes of the Mössbauer spectra being reproduced by a stochastic two-state relaxation model. The dynamics of the transition are determined by values of the rate constant k_{IL} between 4.31×10^6 and 6.09×10^6 s^{-1}. The temperature dependence is described by an Arrhenius equation with the activation energies $\Delta E_{IL} = 0.32$ kJ mol^{-1} and $\Delta E_{LI} = 4.23$ kJ mol^{-1} for the IS → LS and LS → IS conversion, respectively. The corresponding frequency factors are $A_{IL} = 6.9 \times 10^6$ s^{-1} and $A_{LI} \sim 63.7 \times 10^6$ s^{-1}. Shifts of the peak profiles of X-ray diffraction depend linearly on μ_{eff}^2 showing that the transition is closely associated with a modification of unit cell dimensions.

Introduction

Nitrosyl iron complexes [Fe(J·R)NO] where H_2(J·R) denotes a quadridentate Jäger-type ligand[4] have been reported by Numata et al.[5] On the basis of magnetic studies over the temperature range 80-300 K, it was suggested that the two complexes where R = ph and mph (ph = *o*-phenylene, mph = 4-methyl-*o*-phenylene) are involved in a spin-state transition. According to the data, the transition appears to be of the continuous type.

Spin-state transitions between intermediate-spin (IS, $S = {}^3/_2$) and low-spin (LS, $S = {}^1/_2$) states in mononitrosyl iron complexes have been reported previously. The transition in [Fe(salen)NO] where H_2salen = *N*,*N*′-ethylenebis(salicylideneamine) occurs at $T_c = 175$ K and shows a discontinuous character.[6,7] The structure changes associated with the transition are moderate. Studies[8] at 296 and 98 K demonstrate that the average distance between the Fe atom and the N atoms of the salen ligand as well as the distance between Fe and the mean plane of the coordinating N and O atoms decreases by about 0.10 Å in the course of the IS → LS conversion. Simultaneously, the Fe-N-O bond angle decreases from 147 to 127°. Individual Mössbauer spectra corresponding to the $S = {}^3/_2$ and $S = {}^1/_2$ states have been observed. Consequently, the transition is slow on the Mössbauer effect time scale, the relaxation time for the spin conversion being greater than about 1×10^{-7} s. The spin-state transition in the analogous [Fe(salphen)NO] where H_2salphen = *N*,*N*′-*o*-phenylenebis(salicylideneamine) occurs at $T_c \simeq 181$ K, the electronic relaxation between the two spin states being rapid with a relaxation time $\tau \lesssim 1 \times 10^{-8}$ s.[9-11] A

(1) Institut für Physikalische und Theoretische Chemie, University of Erlangen-Nürnberg.
(2) Physikalisches Institut, University of Erlangen-Nürnberg.
(3) University of Surrey.
(4) Wolf, L.; Jäger, E. G. *Z. Anorg. Allg. Chem.* **1966**, *346*, 76.
(5) Numata, Y.; Kubokura, K.; Nonaka, Y.; Okawa, H.; Kida, S. *Inorg. Chim. Acta* **1980**, *43*, 193.
(6) Earnshaw, A.; King, E. A.; Larkworthy, L. F. *J. Chem. Soc. A* **1969**, 2459.
(7) Wells, F. V.; McCann, S. W.; Wickman, H. H.; Kessel, S. L.; Hendrickson, D. N.; Feltham, R. D. *Inorg. Chem.* **1982**, *21*, 2306.
(8) Haller, K. J.; Johnson, P. L.; Feltham, R. D.; Enemark, J. H.; Ferraro, J. R.; Basile, L. J. *Inorg. Chim. Acta* **1979**, *33*, 119.
(9) Fitzsimmons, B. W.; Larkworthy, L. F.; Rogers, K. A. *Inorg. Chim. Acta* **1980**, *44*, L 53.
(10) König, E.; Ritter, G.; Waigel, J.; Larkworthy, L. F.; Thompson, R. M. *Inorg. Chem.* **1987**, *26*, 1563.

0020-1669/92/1331-1196$03.00/0